Topics in Boundary Element Research

Edited by
C. A. Brebbia

Volume 3

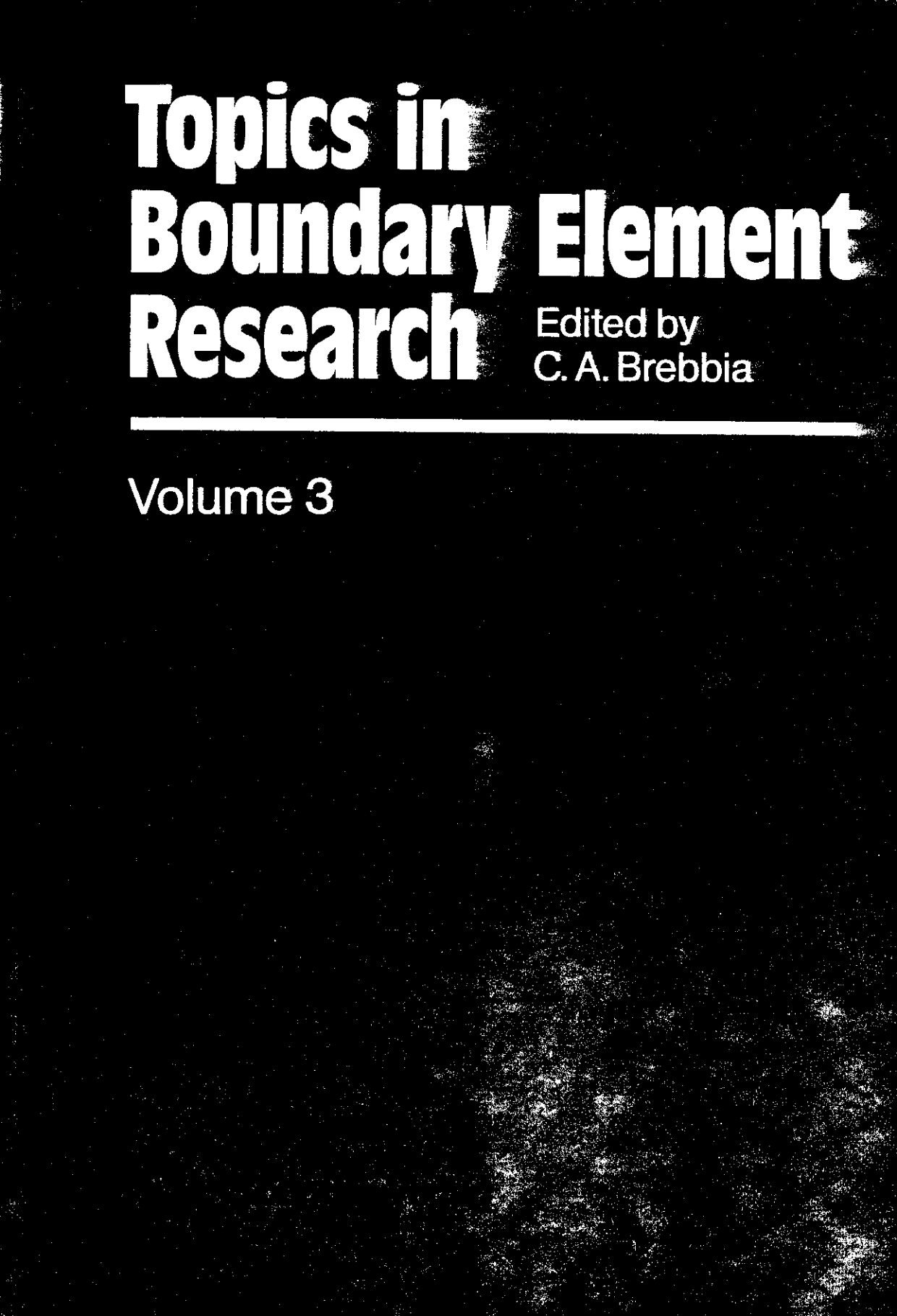

Chapter 7

Complex Variable Boundary Elements in Computational Mechanics

by T. V. Hromadka

7.1 Introduction

A new and exciting numerical approach to solving two-dimensional potential problems is obtained by use of the Cauchy integral equation for analytic functions. The resulting integral equation is readily solvable by computer, and produces a pair of two-dimensional conjugate harmonic functions which satisfy the Laplace equation over the problem domain.

Of special interest, however, are the approximation error evaluation techniques afforded by the Complex Variable Boundary Element Method (CVBEM). One especially useful technique develops an approximate boundary where the CVBEM solution satisfies the local boundary conditions continuously. Error analysis and reduction then proceeds by the addition of nodal points to the problem boundary where discrepancy between the approximate and problem boundaries is seen to be large.

In this chapter, the CVBEM will be developed in detail with special attention paid to linear and constant basis functions specified on the problem boundary. Generalization to higher order basis functions is also included. Approximation error evaluation techniques are reviewed, with a focus upon the approximate boundary method.

7.2 A Complex Variable Boundary Element Approximation Model

Let Ω be a simply connected domain with an associated simple closed contour boundary Γ. Assume that Γ is a polygonal line composed of V straight line segments and vertices (Fig. 1). Let $\omega(z) = \phi(z) + \mathrm{i}\,\psi(z)$ be a complex variable function which is analytic on $\Omega \cup \Gamma$ where ϕ and ψ are the state variable (or potential) and stream functions, respectively. Then the real variable functions composing $\omega(z)$ are related by the Cauchy-Riemann equations on $\Omega \cup \Gamma$:

$$\frac{\partial \phi}{\partial x} = \frac{\partial \psi}{\partial y}, \quad \frac{\partial \phi}{\partial y} = -\frac{\partial \psi}{\partial x}. \tag{1}$$

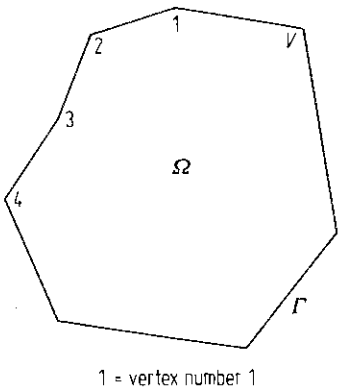

Fig. 1. Domain $\Omega \cup \Gamma$

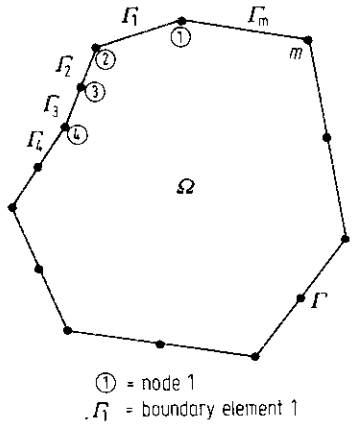

Fig. 2. Nodal point distribution on Γ

Consequently, ϕ and ψ are harmonic functions for $z \in \Omega \cup \Gamma$ such that

$$\frac{\partial^2 \phi}{\partial x^2} + \frac{\partial^2 \phi}{\partial y^2} = 0, \quad \frac{\partial^2 \psi}{\partial x^2} + \frac{\partial^2 \psi}{\partial y^2} = 0. \tag{2}$$

Define on Γ a partition of nodal points $\{z_j, j = 1, 2, \ldots, m\}$ such that at least at each boundary vertex there is a nodal point, i.e. $m \geqq V$. The nodal points are numbered (sequentially from 1) in a counterclockwise direction around Γ (Fig. 2).

At each nodal point z_j, define the symbols $\bar{\phi}_j$ and $\bar{\psi}_j$ to represent specified nodal values where each value is a real number. Similarly, let ϕ_j and ψ_j be notation for the values of $\phi(z_j)$ and $\psi(z_j)$ respectively, $j = 1, 2, \ldots, m$.

Define 2-node boundary elements Γ_j on Γ by

$$\Gamma = \bigcup_{j=1}^{m} \Gamma_j, \tag{3}$$

where

$$\Gamma_j = \{z \in \Gamma: z = z_j(1 - s) + z_{j+1}\, s, 0 \leqq s \leqq 1\} \quad \text{and} \quad \Gamma_j \cap \Gamma_{j+1} = z_{j+1}.$$

The numbering of boundary elements follows the nodal point numbering scheme shown in Fig. 2.

A continuous global trial function $G_1(z)$ is defined on Γ by

$$G_1(z) = \sum_{j=1}^{m} N_j(z)\, \bar{\phi}_j + \mathrm{i} \sum_{j=1}^{m} N_j(z)\, \bar{\psi}_j \tag{4}$$

where a typical basis function is defined for nodal point j by

$$N_j(z) = \begin{cases} (z - z_{j-1})/(z_j - z_{j-1}), & z \in \Gamma_{j-1} \\ (z_{j+1} - z)/(z_{j+1} - z_j), & z \in \Gamma_j \\ 0, & z \notin \Gamma_{j-1} \cup \Gamma_{j+1} \end{cases} \tag{5}$$

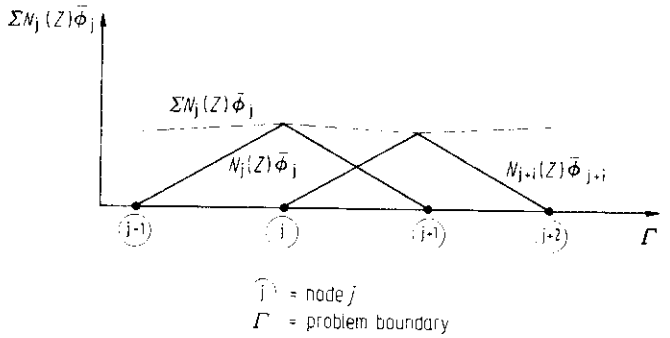

Fig. 3. The linear basis function relationship to the global trial function

Figure 3 shows the linear basis function and its relation to the global trial function $G_1(z)$. The global trial function is seen to be continuous on Γ and $G_1(z_j) = \bar{\phi}_j + \mathrm{i}\,\bar{\psi}_j$, $j = 1, 2, \ldots, m$.

An approximation function (an H_1 approximation function) can be developed by defining

$$\hat{\omega}(z) = \frac{1}{2\pi\,\mathrm{i}} \int_{\Gamma} \frac{G_1(\zeta)\,d\zeta}{\zeta - z}, \quad z \in \Omega \tag{6}$$

where z is in the interior of Ω and not on the boundary Γ, and contour integration is in the positive sense.

The $\hat{\omega}(z)$ approximation function will be shown in Sect. 2 to be analytic in Ω and therefore has the property that its real $\hat{\phi}(z)$ and imaginary $\hat{\psi}(z)$ components satisfy the two-dimensional Laplace equation in Ω. The numerical modeling strategy is to try to determine a $\hat{\omega}(z)$ such that $\hat{\omega}(z)$ is arbitrarily close to $\omega(z)$ values for all boundary points $z \in \Gamma$. To develop such an approximator, $\hat{\omega}(z)$ is written in terms of boundary elements Γ_j by

$$\hat{\omega}(z_0) = \frac{1}{2\pi\,\mathrm{i}} \int_{\bigcup_{j=1}^{m} \Gamma_j} \frac{G_1(\zeta)\,d\zeta}{\zeta - z_0}$$

$$= \frac{1}{2\pi\,\mathrm{i}} \sum_{j=1}^{m} \int_{\Gamma_j} \frac{G_1(\zeta)\,d\zeta}{\zeta - z_0}; \quad z_0 \in \Omega, \quad z_0 \notin \Gamma \tag{7}$$

On each Γ_j, $G_1(z)$ is simplified to

$$G_1(z) = N_j\,\bar{\omega}_j + N_{j+1}\,\bar{\omega}_{j+1} = (N_j\,\bar{\phi}_j + N_{j+1}\,\bar{\phi}_{j+1}) + \mathrm{i}\,(N_j\,\bar{\psi}_j + N_{j+1}\,\bar{\psi}_{j+1}), \quad z \in \Gamma_j \tag{8}$$

where $\bar{\omega}_j = \bar{\phi}_j + \mathrm{i}\,\bar{\psi}_j$, and N_j is used for a shorthand notation for the $N_j(z)$ function. Using (8) the contribution to $\hat{\omega}(z_0)$ from each boundary element Γ_j can be calculated by

$$\int_{\Gamma_j} \frac{G_1(\zeta)\,d\zeta}{\zeta - z_0} = \int_{\Gamma_j} \frac{[(z_{j+1} - \zeta)\,\bar{\omega}_j + (\zeta - z_j)\,\bar{\omega}_{j+1}]/(z_{j+1} - z_j)\,d\zeta}{\zeta - z_0}; \quad z_0 \in \Omega, \; z_0 \notin \Gamma_j \tag{9}$$

The above equation can be simplified by

$$\int_{\Gamma_j} \frac{G_1(\zeta)\,d\zeta}{\zeta - z_0} = \frac{(z_{j+1}\bar{\omega}_j - z_j\bar{\omega}_{j+1})}{(z_{j+1} - z_j)} \int_{\Gamma_j} \frac{d\zeta}{\zeta - z_0} + \frac{(\bar{\omega}_{j+1} - \bar{\omega}_j)}{(z_{j+1} - z_j)} \int_{\Gamma_j} \frac{\zeta\,d\zeta}{\zeta - z_0}$$

$$\int_{\Gamma_j} \frac{\zeta\,d\zeta}{\zeta - z_0} = \int_{\Gamma_j} \frac{(\zeta - z_0)\,d\zeta}{\zeta - z_0} + \int_{\Gamma_j} \frac{z_0\,d\zeta}{\zeta - z_0} = (z_{j+1} - z_j) + z_0 \int_{\Gamma_j} \frac{d\zeta}{\zeta - z_0}$$

$$\int_{\Gamma_j} \frac{d\zeta}{\zeta - z_0} = \ln(\zeta - z_0)\Big|_{z_j}^{z_{j+1}} = \ln\left|\frac{z_{j+1} - z_0}{z_j - z_0}\right| + \mathrm{i}\,\theta(j+1, j)$$

where $\theta(j+1, j)$ is the central angle between the straight line segments joining points z_j and z_{j+1} to central point $z_0 \in \Omega$ (Fig. 4).

Using the above integrations

$$\int_{\Gamma_j} \frac{G_1(\zeta)\,d\zeta}{\zeta - z_0} = \bar{\omega}_{j+1} - \bar{\omega}_j + \bar{\omega}_{j+1}\frac{(z_0 - z_j)}{(z_{j+1} - z_j)}h_j - \bar{\omega}_j\frac{(z_0 - z_{j+1})}{(z_{j+1} - z_j)}h_j \tag{10}$$

where $h_j = \ln(|z_{j+1} - z_0|/|z_j - z_0|) + \mathrm{i}\,\theta(j+1, j)$. The complex value of $\hat{\omega}(z_0)$ is determined as the sum of each Γ_j contribution by

$$2\pi\,\mathrm{i}\,\hat{\omega}(z_0) = \sum_{j=1}^{m}(\bar{\omega}_{j+1} - \bar{\omega}_j) + \sum_{j=1}^{m}[\bar{\omega}_{j+1}(z_0 - z_j) - \bar{\omega}_j(z_0 - z_{j+1})]\,h_j/(z_{j+1} - z_j) \tag{11}$$

where in (11) it is understood that $\bar{\omega}_{m+1} \equiv \bar{\omega}_1$ and $z_{m+1} \equiv z_1$. The first summation term cancels leaving (for linear basis functions)

$$2\pi\,\mathrm{i}\,\hat{\omega}(z_0) = \sum_{j=1}^{m}[\bar{\omega}_{j+1}(z_0 - z_j) - \bar{\omega}_j(z_0 - z_{j+1})]\,h_j/(z_{j+1} - z_j). \tag{12}$$

The above relationship can be written as a complex function

$$\hat{\omega}(z_0) = \hat{\phi}(z_0) + \mathrm{i}\,\hat{\psi}(z_0) \tag{13}$$
$$= \hat{\phi}(z_0, \bar{\phi}_1, \bar{\phi}_2, \ldots, \bar{\phi}_m, \bar{\psi}_1, \bar{\psi}_2, \ldots, \bar{\psi}_m) + \mathrm{i}\,\hat{\psi}(z_0, \bar{\phi}_1, \bar{\phi}_2, \ldots, \bar{\phi}_m, \bar{\psi}_1, \bar{\psi}_2, \ldots, \bar{\psi}_m),$$

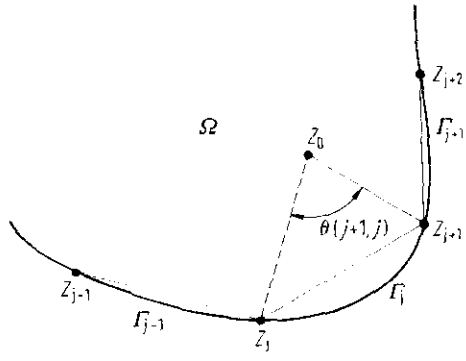

Fig. 4. Nodal point geometry

where z_0 is any point in the interior of Ω, and $\hat{\phi}$ and $\hat{\psi}$ are real valued functions representing the real and imaginary components of the complex function $\omega(z)$. Should values of $\bar{\omega}_j = \bar{\phi}_j + \mathrm{i}\,\bar{\psi}_j$ be known at each z_j, $j = 1, 2, \ldots, m$, then (13) defines a complex valued function which is analytic in Ω, and $\hat{\phi}(x, y)$ and $\hat{\psi}(x, y)$ both satisfy the Laplace equation in Ω. If $\hat{\omega}(z) = \omega(z)$ on Γ, then $\hat{\omega}(z) = \omega(z)$ in Ω and $\hat{\omega}(z)$ is the solution to the boundary value problem.

The usual problem in engineering applications is that only one of the specified nodal value pair $(\bar{\phi}_j, \bar{\psi}_j)$ is known at each z_j and, consequently, part of the modeling task is to evaluate unknown nodal values. A method of developing such an approximation function is to evaluate $\hat{\omega}(z)$ arbitrarily close to each nodal point and in turn, generate an implicit expression of the unknown nodal variable as a function of all the unknown variables. The result is m equations for m unknown nodal values which can be solved by the usual matrix techniques.

The evaluated nodal values are then used along with the original set of known nodal values to complete the definition of the $\hat{\omega}(z)$ approximation function on $\Omega \cup \Gamma$.

For example, suppose that m nodal points are defined on Γ, and $\bar{\psi}_j$ is known for $j = 1, 2, \ldots, k$ where $(0 < k < m)$ and $\bar{\phi}_j$ is known for the remaining nodes $j = (k+1), \ldots, m$. Two methods of generating the unknown nodal values are provided by the following matrix systems:

Case I

$$\begin{aligned}
\bar{\psi}_1 &\equiv \hat{\psi}(z_1^-) = \hat{\psi}(z_1^-, \bar{\phi}_1, \ldots, \bar{\phi}_m, \bar{\psi}_1, \ldots, \bar{\psi}_m) \\
&\vdots \\
\bar{\psi}_k &\equiv \hat{\psi}(z_k^-) = \hat{\psi}(z_k^-, \bar{\phi}_1, \ldots, \bar{\phi}_m, \bar{\psi}_1, \ldots, \bar{\psi}_m) \\
\bar{\phi}_{k+1} &\equiv \hat{\phi}(z_{k+1}^-) = \hat{\phi}(z_{k+1}^-, \bar{\phi}_1, \ldots, \bar{\phi}_m, \bar{\psi}_1, \ldots, \bar{\psi}_m) \\
&\vdots \\
\bar{\phi}_m &\equiv \hat{\phi}(z_m^-) = \hat{\phi}(z_m^-, \bar{\phi}_1, \ldots, \bar{\phi}_m, \bar{\psi}_1, \ldots, \bar{\psi}_m).
\end{aligned} \tag{14}$$

Case II

$$\begin{aligned}
\bar{\phi}_1 &\equiv \hat{\phi}(z_1^-) = \hat{\phi}(z_1^-, \bar{\phi}_1, \ldots, \bar{\phi}_m, \bar{\psi}_1, \ldots, \bar{\psi}_m) \\
\bar{\phi}_2 &\equiv \hat{\phi}(z_2^-) = \hat{\phi}(z_2^-, \bar{\phi}_1, \ldots, \bar{\phi}_m, \bar{\psi}_1, \ldots, \bar{\psi}_m) \\
&\vdots \\
\bar{\phi}_k &\equiv \hat{\phi}(z_k^-) = \hat{\phi}(z_k^-, \bar{\phi}_1, \ldots, \bar{\phi}_m, \bar{\psi}_1, \ldots, \bar{\psi}_m) \\
\bar{\psi}_{k+1} &\equiv \hat{\psi}(z_{k+1}^-) = \hat{\psi}(z_{k+1}^-, \bar{\phi}_1, \ldots, \bar{\phi}_m, \bar{\psi}_1, \ldots, \bar{\psi}_m) \\
&\vdots \\
\bar{\psi}_m &\equiv \hat{\psi}(z_m^-) = \hat{\psi}(z_m^-, \bar{\phi}_1, \ldots, \bar{\phi}_m, \bar{\psi}_1, \ldots, \bar{\psi}_m)
\end{aligned} \tag{15}$$

where z_j^- indicates a point in Ω which is arbitrary close to boundary node coordinate z_j. Solution of both matrix systems will result in different $\hat{\omega}(z)$ function definitions. The case I matrix system produces values for the unknown nodal values such that

$$\hat{\omega}(z_j) = \hat{\phi}(z_j) + \mathrm{i}\,\hat{\psi}(z_j) = \begin{cases} \hat{\phi}(z_j) + \mathrm{i}\,\bar{\psi}_j, & j = 1, 2, \ldots, k \\ \bar{\phi}_j + \mathrm{i}\,\hat{\psi}(z_j), & j = k+1, \ldots, m \end{cases} \tag{16}$$

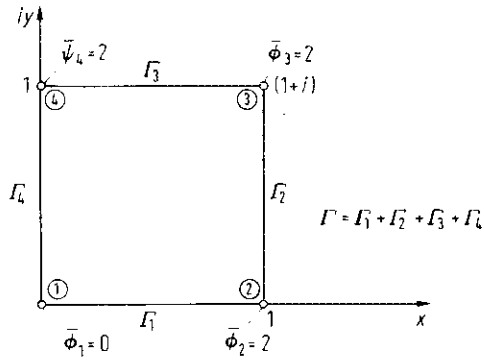

Fig. 5. Problem definition for example. ①, node number 1; ○, nodal point on Γ; Γ_1, boundary element number 1

whereas the case II system results in nodal values which do not necessarily agree with the known specified nodal values.

Example 1. A simple example problem will be used to construct a CVBEM approximation function $\hat{\omega}(z)$. Figure 5 shows the assumed problem geometry and the known speficied nodal point values on Γ. The true solution to the boundary value problem is $\omega(z) = 2z$. The objective is to determine the unknown nodal values of $\{\bar{\psi}_1, \bar{\psi}_2, \bar{\psi}_3, \bar{\phi}_4\}$ and develop an approximation function $\hat{\omega}(z)$ on $\Omega \cup \Gamma$.

For node 1, (12) can be used to develop the nodal equation for a point z_1^- close to z_1 by

$$2\pi \mathrm{i}\, \hat{\omega}(z_1^-) = \sum_{j=1}^{4} [\bar{\omega}_{j+1}(z_1^- - z_j) - \bar{\omega}_j(z_1^- - z_{j+1})]\, h_j/(z_{j+1} - z_j).$$

Letting z_1^- be the complex value $\varepsilon_x + \mathrm{i}\,\varepsilon_y$ (where ε_x and ε_y are both positive real numbers) and expanding the nodal equation for z_1^- gives

$$\begin{aligned} 2\pi \mathrm{i}\, \hat{\omega}(z_1^-) = {} & [\bar{\omega}_2(\varepsilon_x + \mathrm{i}\,\varepsilon_y) - \bar{\omega}_1(\varepsilon_x + \mathrm{i}\,\varepsilon_y - 1)]\, h_1/(1) \\ & + [\bar{\omega}_3(\varepsilon_x + \mathrm{i}\,\varepsilon_y - 1) - \bar{\omega}_2(\varepsilon_x + \mathrm{i}\,\varepsilon_y - 1 - \mathrm{i})]\, h_2/(\mathrm{i}) \\ & + [\bar{\omega}_4(\varepsilon_x + \mathrm{i}\,\varepsilon_y - 1 - \mathrm{i}) - \bar{\omega}_3(\varepsilon_x + \mathrm{i}\,\varepsilon_y - \mathrm{i})]\, h_3/(-1) \\ & + [\bar{\omega}_1(\varepsilon_x + \mathrm{i}\,\varepsilon_y - \mathrm{i}) - \bar{\omega}_4(\varepsilon_x + \mathrm{i}\,\varepsilon_y)]\, h_4/(-\mathrm{i}). \end{aligned}$$

From Fig. 6,

$$h_1 = \ln \left| \frac{1 - \varepsilon_x - \mathrm{i}\,\varepsilon_y}{-\varepsilon_x - \mathrm{i}\,\varepsilon_y} \right| + \mathrm{i}\,\theta(2, 1)$$

$$h_2 = \ln \left| \frac{1 + \mathrm{i} - \varepsilon_x - \mathrm{i}\,\varepsilon_y}{1 - \varepsilon_x - \mathrm{i}\,\varepsilon_y} \right| + \mathrm{i}\,\theta(3, 2)$$

$$h_3 = \ln \left| \frac{\mathrm{i} - \varepsilon_x - \mathrm{i}\,\varepsilon_y}{1 + \mathrm{i} - \varepsilon_x - \mathrm{i}\,\varepsilon_y} \right| + \mathrm{i}\,\theta(4, 3)$$

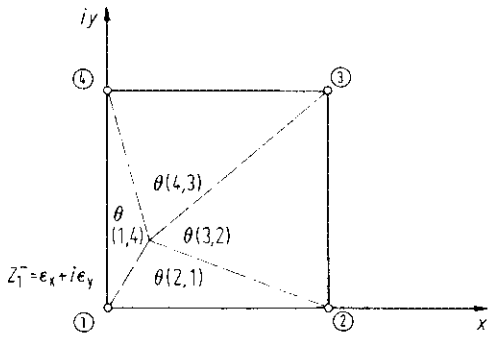

Fig. 6. Geometric values for nodal point ①

$$h_4 = \ln \left| \frac{-\varepsilon_x - \mathrm{i}\,\varepsilon_y}{\mathrm{i} - \varepsilon_x - \mathrm{i}\,\varepsilon_y} \right| + \mathrm{i}\,\theta(1,4).$$

All of the above terms are continuous functions for z_1^- in the interior of Ω; that is, for $\varepsilon_x > 0$ and $\varepsilon_y > 0$. As z_1^- approaches z_1, however, several terms can be evaluated as a limit. These limiting values are as fóllows:

$$\lim_{z_1^- \to z_1} 2\pi\,\mathrm{i}\,\hat{\omega}(z_1^-) = \lim_{\substack{\varepsilon_x \to 0 \\ \varepsilon_y \to 0}} 2\pi\,\mathrm{i}\,\hat{\omega}(\varepsilon_x + \mathrm{i}\,\varepsilon_y)$$

$$= [0 - \bar{\omega}_1(-1)] \left(\lim_{\substack{\varepsilon_x \to 0 \\ \varepsilon_y \to 0}} \ln \left| \frac{1 - \varepsilon_x - \mathrm{i}\,\varepsilon_y}{-\varepsilon_x - \mathrm{i}\,\varepsilon_y} \right| + \mathrm{i}\,\theta(2,1) \right) \Big/ (1)$$

$$+ [\bar{\omega}_3(-1) - \bar{\omega}_2(-1-\mathrm{i})] \left(\ln \left| \frac{1+\mathrm{i}}{1} \right| + \frac{\pi}{4}\mathrm{i} \right) \Big/ (\mathrm{i})$$

$$+ [\bar{\omega}_4(-1-\mathrm{i}) - \bar{\omega}_3(-\mathrm{i})] \left(\ln \left| \frac{\mathrm{i}}{1+\mathrm{i}} \right| + \frac{\pi}{4}\mathrm{i} \right) \Big/ (-1)$$

$$+ [\bar{\omega}_1(-\mathrm{i}) - 0] \left(\lim_{\substack{\varepsilon_x \to 0 \\ \varepsilon_y \to 0}} \ln \left| \frac{-\varepsilon_x - \mathrm{i}\,\varepsilon_y}{\mathrm{i} - \varepsilon_x - \mathrm{i}\,\varepsilon_y} \right| + \mathrm{i}\,\theta(1,4) \right) \Big/ (-\mathrm{i})$$

Simplifying terms,

$$\lim_{\substack{\varepsilon_x \to 0 \\ \varepsilon_y \to 0}} 2\pi\,\mathrm{i}\,\hat{\omega}(\varepsilon_x + \mathrm{i}\,\varepsilon_y) = \bar{\omega}_1 \left(\lim_{\substack{\varepsilon_x \to 0 \\ \varepsilon_y \to 0}} \ln \left| 1 - \varepsilon_x - \mathrm{i}\,\varepsilon_y \right| - \lim_{\substack{\varepsilon_x \to 0 \\ \varepsilon_y \to 0}} \ln \left| -\varepsilon_x - \mathrm{i}\,\varepsilon_y \right| + \mathrm{i}\,\theta(2,1) \right)$$

$$+ [-\bar{\omega}_3 + \bar{\omega}_2(1+\mathrm{i})](-\mathrm{i}\ln\sqrt{2} + \tfrac{\pi}{4})$$

$$+ [\bar{\omega}_4(1+\mathrm{i}) - \bar{\omega}_3\,\mathrm{i}](-\ln\sqrt{2} + \tfrac{\pi}{4}\mathrm{i})$$

$$+ \bar{\omega}_1 \left(\lim_{\substack{\varepsilon_x \to 0 \\ \varepsilon_y \to 0}} \ln \left| -\varepsilon_x - \mathrm{i}\,\varepsilon_y \right| - \lim_{\substack{\varepsilon_x \to 0 \\ \varepsilon_y \to 0}} \ln \left| \mathrm{i} - \varepsilon_x - \mathrm{i}\,\varepsilon_y \right| + \mathrm{i}\,\theta(1,4) \right).$$

In the above expression, the singularity difficulties due to the term $\ln|\varepsilon_x + \mathrm{i}\,\varepsilon_y|$ sum to zero. Additionally, from Fig. 6, $(\theta(1,4) + \theta(2,1)) = 2\pi - (\theta(4,3) + \theta(3,2))$ and the limiting value of these angles are determined to be

$$\lim_{\substack{\varepsilon_x \to 0 \\ \varepsilon_y \to 0}} (\theta(1,4) + \theta(2,1)) = 2\pi - (\tfrac{\pi}{2}) = \frac{3\pi}{2}.$$

Defining $\lim_{z_1^- \to z_1} 2\pi\,\mathrm{i}\,\hat{\omega}(z_1^-) = 2\pi\,\mathrm{i}\,\hat{\omega}(z_1)$ gives the following new nodal equation for node z_1 as the limiting value

$$2\pi\,\mathrm{i}\,\hat{\omega}(z_1) = \bar{\omega}_1\left(\frac{3\pi}{2}\,\mathrm{i}\right) + \bar{\omega}_2[(\tfrac{\pi}{4} + \ln\sqrt{2}) + \mathrm{i}\,(\tfrac{\pi}{4} - \ln\sqrt{2})] + \bar{\omega}_3[\mathrm{i}\ln 2] + \bar{\omega}_4[(-\tfrac{\pi}{4} - \ln\sqrt{2}) + \mathrm{i}\,(\tfrac{\pi}{4} - \ln\sqrt{2})].$$

Separating the nodal equation into real and imaginary components determines two nodal value equations,

$$-2\pi\,\hat{\psi}(z_1) = \left(-\frac{3\pi}{2}\right)\bar{\psi}_1 + (\tfrac{\pi}{4} + \ln\sqrt{2})\,\bar{\phi}_2 - (\tfrac{\pi}{4} - \ln\sqrt{2})\,\bar{\psi}_2 + (-\ln 2)\,\bar{\psi}_3 - (-\tfrac{\pi}{4} - \ln\sqrt{2})\,\bar{\phi}_4 - (\tfrac{\pi}{4} - \ln\sqrt{2})\,\bar{\psi}_4$$

$$2\pi\,\hat{\phi}(z_1) = \frac{3\pi}{2}\,\bar{\phi}_1 + (\tfrac{\pi}{4} + \ln\sqrt{2})\,\bar{\psi}_2 + (\tfrac{\pi}{4} - \ln\sqrt{2})\,\bar{\phi}_2 + (\ln 2)\,\bar{\phi}_3 + (\tfrac{\pi}{4} - \ln\sqrt{2})\,\bar{\psi}_4 + (-\tfrac{\pi}{4} - \ln\sqrt{2})\,\bar{\phi}_4.$$

Similar pairs of nodal equations can be determined for the remaining nodal values at z_2, z_3 and z_4 by rotating $\Omega \cup \Gamma$ so that each node in turn occupies the already studied $z_1 = 0 + 0\,\mathrm{i}$ location

For this example problem, define constant coefficients

$$\gamma_1 = \tfrac{3}{4}, \quad \gamma_2 = \tfrac{1}{8} + \frac{\ln\sqrt{2}}{2\pi}, \quad \gamma_3 = \tfrac{1}{8} - \frac{\ln\sqrt{2}}{2\pi}, \quad \gamma_4 = \frac{\ln 2}{2\pi}.$$

Then the following nodal value equations are determined:

$$\hat{\psi}(z_1) = \gamma_1\,\bar{\psi}_1 - \gamma_2\,\bar{\phi}_2 + \gamma_3\,\bar{\psi}_2 + \gamma_4\,\bar{\psi}_3 + \gamma_2\,\bar{\phi}_4 + \gamma_3\,\bar{\psi}_4$$

$$\hat{\phi}(z_1) = \gamma_1\,\bar{\phi}_1 + \gamma_2\,\bar{\psi}_2 + \gamma_3\,\bar{\phi}_2 + \gamma_4\,\bar{\phi}_3 - \gamma_2\,\bar{\psi}_4 + \gamma_3\,\bar{\phi}_4$$

Note that in the $\psi(z_1)$ equation the coefficients of the $\bar{\phi}_2$ and $\bar{\phi}_4$ terms sum to zero and the coefficients of $\bar{\psi}_1$, $\bar{\psi}_2$, $\bar{\psi}_3$, and $\bar{\psi}_4$ sum to one. A similar result holds for the $\hat{\phi}(z_1)$ equation. The remaining nodal equations are determined as

$$\hat{\psi}(z_2) = \gamma_1\,\bar{\psi}_2 - \gamma_2\,\bar{\phi}_3 + \gamma_3\,\bar{\psi}_3 + \gamma_4\,\bar{\psi}_4 + \gamma_2\,\bar{\phi}_1 + \gamma_3\,\bar{\psi}_1$$

$$\hat{\phi}(z_2) = \gamma_1\,\bar{\phi}_2 + \gamma_2\,\bar{\psi}_3 + \gamma_3\,\bar{\phi}_3 + \gamma_4\,\bar{\phi}_4 - \gamma_2\,\bar{\psi}_1 + \gamma_3\,\bar{\phi}_1$$

$$\hat{\psi}(z_3) = \gamma_1\,\bar{\psi}_3 - \gamma_2\,\bar{\phi}_4 + \gamma_3\,\bar{\psi}_4 + \gamma_4\,\bar{\psi}_1 + \gamma_2\,\bar{\phi}_2 + \gamma_3\,\bar{\psi}_2$$

$$\hat{\phi}(z_3) = \gamma_1\,\bar{\phi}_3 + \gamma_2\,\bar{\psi}_4 + \gamma_3\,\bar{\phi}_4 + \gamma_4\,\bar{\phi}_1 - \gamma_2\,\bar{\psi}_2 + \gamma_3\,\bar{\phi}_2$$

$$\hat{\psi}(z_4) = \gamma_1\,\bar{\psi}_4 - \gamma_2\,\bar{\phi}_1 + \gamma_3\,\bar{\psi}_1 + \gamma_4\,\bar{\psi}_2 + \gamma_2\,\bar{\phi}_3 + \gamma_3\,\bar{\psi}_3$$

$$\hat{\phi}(z_4) = \gamma_1\,\bar{\phi}_4 + \gamma_2\,\bar{\psi}_1 + \gamma_3\,\bar{\phi}_1 + \gamma_4\,\bar{\phi}_2 - \gamma_2\,\bar{\psi}_3 + \gamma_3\,\bar{\phi}_3.$$

To solve for the unknown nodal values of $\bar{\psi}_1$, $\bar{\psi}_2$, $\bar{\psi}_3$, and $\bar{\psi}_4$, two methods are possible. Determine a case I matrix system such as given in (14) or determine a case II matrix system such as given in (15).

The case I matrix system sets the known nodal values equal to the approximation function values by forcing

Case I

$$\begin{Bmatrix} \bar{\phi}_1 \\ \bar{\phi}_2 \\ \bar{\phi}_3 \\ \bar{\psi}_4 \end{Bmatrix} \equiv \begin{Bmatrix} \hat{\phi}(z_1) \\ \hat{\phi}(z_2) \\ \hat{\phi}(z_3) \\ \bar{\psi}(z_4) \end{Bmatrix}$$

which gives

$$\begin{Bmatrix} \bar{\phi}_1 \\ \bar{\phi}_2 \\ \bar{\phi}_3 \\ \bar{\psi}_4 \end{Bmatrix} = \begin{bmatrix} 0 & \gamma_2 & 0 & \gamma_3 \\ -\gamma_2 & 0 & \gamma_2 & \gamma_4 \\ 0 & -\gamma_2 & 0 & \gamma_3 \\ \gamma_3 & \gamma_4 & \gamma_3 & 0 \end{bmatrix} \begin{Bmatrix} \bar{\psi}_1 \\ \bar{\psi}_2 \\ \bar{\psi}_3 \\ \bar{\phi}_4 \end{Bmatrix} + \begin{Bmatrix} \gamma_1 \bar{\phi}_1 + \gamma_3 \bar{\phi}_2 + \gamma_4 \bar{\phi}_3 - \gamma_2 \bar{\psi}_4 \\ \gamma_1 \bar{\phi}_2 + \gamma_3 \bar{\phi}_3 + \gamma_3 \bar{\phi}_1 \\ \gamma_1 \bar{\phi}_3 + \gamma_2 \bar{\psi}_4 + \gamma_4 \bar{\phi}_1 + \gamma_3 \bar{\phi}_2 \\ -\gamma_2 \bar{\phi}_1 + \gamma_2 \bar{\phi}_3 + \gamma_1 \bar{\psi}_4 \end{Bmatrix}$$

or simply

$$\begin{bmatrix} 0 & \gamma_2 & 0 & \gamma_3 \\ -\gamma_2 & 0 & \gamma_2 & \gamma_4 \\ 0 & -\gamma_2 & 0 & \gamma_3 \\ \gamma_3 & \gamma_4 & \gamma_3 & 0 \end{bmatrix} \begin{Bmatrix} \bar{\psi}_1 \\ \bar{\psi}_2 \\ \bar{\psi}_3 \\ \bar{\phi}_4 \end{Bmatrix} = \begin{Bmatrix} 0 \\ \frac{1}{4} + (\ln \sqrt{2})/\pi \\ 0 \\ \frac{1}{4} - (\ln \sqrt{2})/\pi \end{Bmatrix}$$

which has the solution nodal values $\{\bar{\psi}_1, \bar{\psi}_2, \bar{\psi}_3, \bar{\phi}_4\} = \{0, 0, 2, 0\}$.

Similarly, the case II matrix system sets the unknown nodal values equal to the approximation function values by forcing

Case II

$$\begin{Bmatrix} \bar{\psi}_1 \\ \bar{\psi}_2 \\ \bar{\psi}_3 \\ \bar{\phi}_4 \end{Bmatrix} \equiv \begin{Bmatrix} \hat{\psi}(z_1) \\ \hat{\psi}(z_2) \\ \hat{\psi}(z_3) \\ \hat{\phi}(z_4) \end{Bmatrix}$$

which gives

$$\begin{Bmatrix} \bar{\psi}_1 \\ \bar{\psi}_2 \\ \bar{\psi}_3 \\ \bar{\phi}_4 \end{Bmatrix} = \begin{bmatrix} \gamma_1 & \gamma_3 & \gamma_4 & \gamma_2 \\ \gamma_3 & \gamma_1 & \gamma_3 & 0 \\ \gamma_4 & \gamma_3 & \gamma_1 & -\gamma_2 \\ \gamma_2 & 0 & -\gamma_3 & \gamma_1 \end{bmatrix} \begin{Bmatrix} \bar{\psi}_1 \\ \bar{\psi}_2 \\ \bar{\psi}_3 \\ \bar{\phi}_4 \end{Bmatrix} + \begin{bmatrix} -\gamma_2 \bar{\phi}_2 + \gamma_3 \bar{\psi}_4 \\ -\gamma_2 \bar{\phi}_3 + \gamma_4 \bar{\psi}_4 + \gamma_2 \bar{\phi}_1 \\ \gamma_3 \bar{\psi}_4 + \gamma_2 \bar{\phi}_2 \\ \gamma_3 \bar{\phi}_1 + \gamma_4 \bar{\phi}_2 + \gamma_3 \bar{\phi}_3 \end{bmatrix}$$

or simply

$$\begin{bmatrix} (\gamma_1 - 1) & \gamma_3 & \gamma_4 & \gamma_2 \\ \gamma_3 & (\gamma_1 - 1) & \gamma_3 & 0 \\ \gamma_4 & \gamma_3 & (\gamma_1 - 1) & -\gamma_2 \\ \gamma_2 & 0 & -\gamma_3 & (\gamma_1 - 1) \end{bmatrix} \begin{Bmatrix} \bar{\psi}_1 \\ \bar{\psi}_2 \\ \bar{\psi}_3 \\ \bar{\phi}_4 \end{Bmatrix} = \begin{Bmatrix} (\ln 2)/\pi \\ \frac{1}{4} - (\ln 2)/(2\pi) \\ -\frac{1}{2} \\ -\frac{1}{4} - (\ln 2)/(2\pi) \end{Bmatrix}$$

which has the solution nodal values of

$$\{\bar{\psi}_1, \bar{\psi}_2, \bar{\psi}_3, \bar{\phi}_4\} = \{0, 0, 2, 0\}.$$

Because the assumed basis functions for $\phi(\zeta)$ and $\psi(\zeta)$ (with $\zeta \in \Gamma$) are of the same polynomial order as the solution to the boundary value problem, then the approximation function $\hat{\omega}(z)$ must be the exact solution, and $\hat{\omega}(z) = \omega(z)$ for $z \in \Omega \cup \Gamma$.

From this example, the limiting value of $\hat{\omega}(z_j^-)$ as z_j^- approaches node z_j with z_j^- in the interior of Ω is useful in determining nodal equations. Therefore, a general relationship is needed to evaluate this limiting value.

Consider a linear trial function between successive nodes (z_1, z_2) and (z_2, z_3).

Then for $z_0 \in \Omega$ and $\zeta_0 \notin \Gamma$

$$2\pi \mathrm{i}\, \hat{\omega}(z_0) = \int_{z_1}^{z_2} \frac{G_1(\zeta)\, d\zeta}{\zeta - z_0} + \int_{z_2}^{z_3} \frac{G_1(\zeta)\, d\zeta}{\zeta - z_0} + \sum_{z_i \neq z_1, z_2} \int_{z_i}^{z_{i+1}} \frac{G_1(\zeta)\, d\zeta}{\zeta - z_0} \tag{17}$$

Define

$$I = 2\pi \mathrm{i}\, \hat{\omega}(z_0) - \int_{z_1}^{z_2} \frac{G_1(\zeta)\, d\zeta}{\zeta - z_0} - \int_{z_2}^{z_3} \frac{G_1(\zeta)\, d\zeta}{\zeta - z_0}. \tag{18}$$

For the linear basis function assumptions, using (10)

$$I = 2\pi \mathrm{i}\, \hat{\omega}(z_0) - \left[\bar{\omega}_2 - \bar{\omega}_1 + \bar{\omega}_1 \left(\frac{z_2 - z_0}{z_2 - z_1} \right) \ln \left(\frac{z_2 - z_0}{z_1 - z_0} \right) - \bar{\omega}_2 \left(\frac{z_1 - z_0}{z_2 - z_1} \right) \ln \left(\frac{z_2 - z_0}{z_1 - z_0} \right) \right]$$

$$- \left[\bar{\omega}_3 - \bar{\omega}_2 + \bar{\omega}_2 \left(\frac{z_3 - z_0}{z_3 - z_2} \right) \ln \left(\frac{z_3 - z_0}{z_2 - z_0} \right) - \bar{\omega}_3 \left(\frac{z_2 - z_0}{z_3 - z_2} \right) \ln \left(\frac{z_3 - z_0}{z_2 - z_0} \right) \right]. \tag{19}$$

In the limit as z_0 approaches z_2 ($z_0 \in \Omega$, $z_2 \in \Gamma$),

$$\lim_{z_0 \to z_2} I = 2\pi \mathrm{i}\, \hat{\omega}(z_2) - \left[(\bar{\omega}_3 - \bar{\omega}_1) + \bar{\omega}_2 \ln \left(\frac{z_3 - z_2}{z_1 - z_2} \right) \right]. \tag{20}$$

Simplifying,

$$\lim_{z_0 \to z_2} I = 2\pi \mathrm{i}\, \hat{\omega}_2 - (\bar{\omega}_3 - \bar{\omega}_1) + \bar{\omega}_2 \ln \left| \frac{z_1 - z_2}{z_3 - z_2} \right| - \mathrm{i}\,(2\pi - \theta)\, \bar{\omega}_2. \tag{21}$$

Hence, the nodal equation for arbitrary node z_2 in Γ is

$$2\pi \mathrm{i}\, \hat{\omega}_2 = \bar{\omega}_3 - \bar{\omega}_1 + \bar{\omega}_2 \left[\ln \left| \frac{z_3 - z_2}{z_1 - z_2} \right| + \mathrm{i}\,(2\pi - \theta) \right] + \sum_{z_i \neq z_1, z_2} \int_{z_i}^{z_{i+1}} \frac{G_1(\zeta)\, d\zeta}{\zeta - z_0}. \tag{22}$$

7.3 The Analytical Function Defined by the Approximator $\hat{\omega}(z)$

The approximation function $\hat{\omega}(z)$ is defined by the contour integral

$$\hat{\omega}(z) = \frac{1}{2\pi \mathrm{i}} \int_{\Gamma} \frac{G_1(\zeta)\, d\zeta}{\zeta - z}, \quad z \notin \Gamma$$

where Γ is a simple closed contour with simply connected interior Ω, and $z \in \Omega$. Specifically, the usual case is, Γ is a simple closed contour composed of straight line segments and its interior, Ω, has no holes in it (i.e. multiply connected). This type of domain $\Omega \cup \Gamma$ is said to be a member of the set of all such domains, P.

Since $G_1(\zeta)$ is a continuous function for $\zeta \in \Gamma$, then the $\hat{\omega}(z)$ function is analytic on Ω. This important result is proved in the following.

Theorem. Let Γ be a simple closed contour with finite length L. Let $h(\zeta)$ be a continuous function on Γ. Then $\hat{\omega}(z)$ is analytic in the interior of Γ where $\hat{\omega}(z)$ is defined by the contour integral

$$\hat{\omega}(z) = \frac{1}{2\pi i} \int_\Gamma \frac{h(\zeta)}{\zeta - z}\, d\zeta$$

and $\hat{\omega}'(z)$ is given by the integral

$$\hat{\omega}'(z) = \frac{1}{2\pi i} \int_\Gamma \frac{h(\zeta)}{(\zeta - z)^2}\, d\zeta .$$

Proof. Since $|h(\zeta)|$ is continuous on the compact set Γ there exists a real number M such that

$$|h(\zeta)| \leqq M \quad \text{for } \zeta \in \Gamma .$$

Let $z_0 \notin \Gamma$ be arbitrary and set $R = d(z_0, \Gamma)$ the distance from z_0 to the contour Γ. To show that $\hat{\omega}(z)$ is analytic at z_0, it will be shown that the derivative exists at z_0.

Let z be any complex number with $|z - z_0| < R/2$. Then

$$\begin{aligned}
\frac{\hat{\omega}(z) - \hat{\omega}(z_0)}{z - z_0} &= \frac{1}{z - z_0} \frac{1}{2\pi i} \int_\Gamma \left[\frac{h(\zeta)}{\zeta - z} - \frac{h(\zeta)}{\zeta - z_0} \right] d\zeta \\
&= \frac{1}{z - z_0} \frac{1}{2\pi i} \int_\Gamma \frac{z - z_0}{(\zeta - z)(\zeta - z_0)} h(\zeta)\, d\zeta \\
&= \frac{1}{2\pi i} \int_\Gamma \frac{h(\zeta)}{(\zeta - z)(\zeta - z_0)}\, d\zeta .
\end{aligned}$$

Expanding these equations gives

$$\begin{aligned}
\left| \frac{\hat{\omega}(z) - \hat{\omega}(z_0)}{z - z_0} - \frac{1}{2\pi i} \int_\Gamma \frac{h(\zeta)}{(\zeta - z_0)^2}\, d\zeta \right| &= \frac{1}{2\pi} \left| \int_\Gamma \left[\frac{h(\zeta)}{(\zeta - z)(\zeta - z_0)} - \frac{h(\zeta)}{(\zeta - z_0)^2} \right] d\zeta \right| \\
&= \frac{1}{2\pi} \left| \int_\Gamma \frac{z - z_0}{(\zeta - z)(\zeta - z_0)^2} h(\zeta)\, d\zeta \right| \\
&\leqq \frac{1}{2\pi} \int_\Gamma \frac{|z - z_0|}{|\zeta - z|\,|\zeta - z_0|^2} |h(\zeta)|\, |d\zeta| \\
&\leqq \frac{1}{2\pi} \int_\Gamma \frac{|z - z_0|}{R(R/2)^2} M\, |d\zeta| \\
&\leqq \frac{2M|z - z_0|}{\pi R^3} \int_\Gamma |d\zeta| \\
&\leqq \frac{2ML}{\pi R^3} |z - z_0| .
\end{aligned}$$

Since the right side goes to 0 as $z \to z_0$,

$$\lim_{z \to z_0} \frac{\hat{\omega}(z) - \hat{\omega}(z_0)}{z - z_0} = \frac{1}{2\pi i} \int_\Gamma \frac{h(\zeta)}{(\zeta - z_0)^2} d\zeta$$

and $\hat{\omega}(z_0)$ is differentiable at any point z_0 not on the contour Γ. Thus, $\hat{\omega}(z)$ is analytic for z_0 in the interior of Γ.

From the above important theorem, it is concluded that the $\hat{\omega}(z)$ approximation function contains real and imaginary functions $\hat{\omega}(z) = \bar{\phi}(z) + i\,\hat{\psi}(z)$ such that $\bar{\phi}(z)$ and $\hat{\psi}(z)$ are both harmonic in Ω. If $\hat{\omega}(z)$ satisfies the boundary conditions which are specified from the function $\omega(z)$, where $\omega(z)$ is analytic on $\Omega \cup \Gamma \in P$, then $\hat{\omega}(z) = \omega(z)$ for $z \in \Omega \cup \Gamma$. However, generally $\hat{\omega}(z) \neq \omega(z)$ for $z \in \Gamma$ and an error function $e(z)$ exists on $\Omega \cup \Gamma$ where

$$e(z) = \omega(z) - \hat{\omega}(z), \quad z \in \Gamma \tag{23}$$

and $e(z)$ is not identically zero on $\Omega \cup \Gamma$. Thus, the numerical modeling objective is to reduce $e(z)$ on $\Omega \cup \Gamma$.

7.4 A Constant Boundary Element Method

A simpler modeling approach than determining a continuous global interpolation function on Γ is to assume that the integration contribution from each element Γ_j is simply

$$\int_{\Gamma_j} \frac{\omega(\zeta)\, d\zeta}{\zeta - z_0} = \bar{\omega}_j \int_{\Gamma_j} \frac{d\zeta}{\zeta - z} \tag{24}$$

where $\bar{\omega}_j$ is a specified value for element Γ_j. In this modeling approach, the nodal points are assumed located at midelement (see Fig. 7).

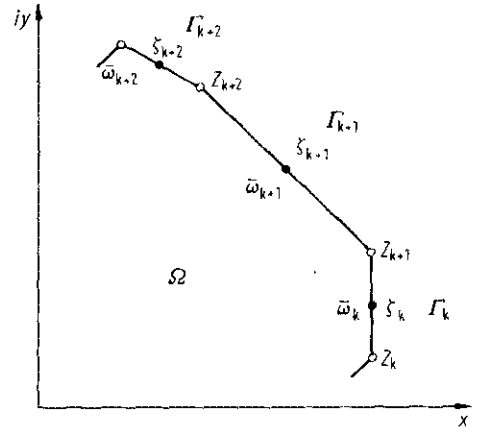

Fig. 7. Constant boundary element geometry. ○, element points; ● nodal point; ζ_k, midelement node on Γ_k

The nodal equation contributions are simply

$$\bar{\omega}_j \int_{\Gamma_j} \frac{d\zeta}{\zeta - \zeta_k} = \bar{\omega}_j \ln\left(\frac{z_{j+1} - \zeta_k}{z_j - \zeta_k}\right) \tag{25}$$

where ζ_k is the coordinate of node k. Letting $d(z_j, \zeta_k)$ be the usual distance function gives

$$\bar{\omega}_j \int \frac{d\zeta}{\zeta - \zeta_k} = \bar{\omega}_j \left[\ln\left(\frac{d(z_{j+1}, \zeta_k)}{d(z_j, \zeta_k)}\right) + \mathrm{i}\, \theta(j+1, j) \right] \tag{26}$$

where $\theta(j+1, j)$ is the central angle between coordinates z_{j+1}, z_j and ζ_k. Thus

$$\bar{\omega}_j \int_{\Gamma_j} \frac{d\zeta}{\zeta - \zeta_k} = \bar{\omega}_j h_j, \quad j \neq k. \tag{27}$$

The limiting value for $j = k$ is given by considering

$$\lim_{z \to \zeta_k} \bar{\omega}_k \int_{\Gamma_k} \frac{d\zeta}{\zeta - z} \tag{28}$$

where z is in the interior of Ω. But

$$\bar{\omega}_k \int_{\Gamma_k} \frac{d\zeta}{\zeta - z} = \bar{\omega}_k \ln\left(\frac{z_{k+1} - z}{z_k - z}\right) \tag{29}$$

where $\zeta_k = (z_{k+1} + z_k)/2$. Let $z = \zeta_k + \varepsilon_x + \mathrm{i}\, \varepsilon_y$, then

$$\bar{\omega}_k \int_{\Gamma_k} \frac{d\zeta}{\zeta - z} = \bar{\omega}_k \ln\left(\frac{(z_{k+1} - z_k)/2 - \varepsilon_x - \mathrm{i}\, \varepsilon_y}{(z_k - z_{k+1})/2 - \varepsilon_x - \mathrm{i}\, \varepsilon_y}\right)$$

and in the limit

$$\lim_{\substack{\varepsilon_x \to 0 \\ \varepsilon_y \to 0}} \int_{\Gamma_k} \frac{d\zeta}{\zeta - z} = \bar{\omega}_k \ln(-1) = \bar{\omega}_k \pi \mathrm{i}.$$

The constant element nodal equation is then

$$2\pi \mathrm{i}\, \hat{\omega}(\zeta_k) = \bar{\omega}_k \pi \mathrm{i} + \sum_{j \neq k} \bar{\omega}_j h_j; \quad k = 1, 2, \ldots, m \tag{30}$$

where it is assumed that m constant boundary elements are used in the model. The development of case I and case II matrix systems follows in an analogous fashion from Sect. 1.

7.5 The Complex Variable Boundary Element Method

The preceding discussions can be generalized to formulate a complex variable boundary element method, or simply the CVBEM.

Let $\Omega \cup \Gamma \in P$. Discretize Γ into m boundary elements Γ_j such that

$$\Gamma = \sum_{j=1}^{m} \Gamma_j$$

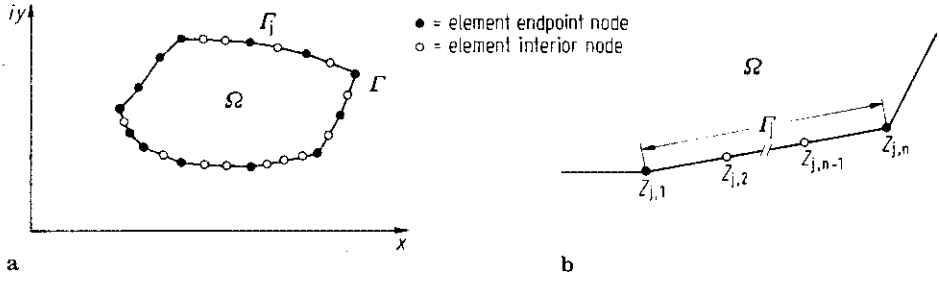

Fig. 8. **a** Boundary discretized into several n-node elements. **b** Detail of element Γ_j

and the intersection of $\Gamma_j \cap \Gamma_{j-1}$ is endpoint of Γ_j and Γ_{j-1}. On each element Γ_j define two or more evenly spaced nodal points. Number each boundary element sequentially from 1 to m along Γ in the counterclockwise direction. Similarly, number the nodal points sequentially from 1 as Γ is transversed in the counterclockwise direction.

A second nodal numbering scheme is as shown in Fig. 8 where the endpoints of an n-node element Γ_j are defined as $z_{j,1}$ and $z_{j,n}$.

Define on each element Γ_j a system of continuous basis functions $N_{j,k}(z)$ such that

$$N_{j,i}(z) = \begin{cases} 1, & z = z_{j,i} \\ 0, & z = z_{j,k}, \quad k \neq i \end{cases} \tag{31}$$

and $N_{j,k}(z) \equiv 0$ for $z \notin \Gamma_j$. The real valued interpolation functions $\alpha_{\phi_j}(z)$ and $\alpha_{\psi_j}(z)$ are defined on Γ_j by

$$\alpha_{\phi_j}(z) = \sum_{k=1}^{n} N_{j,k}(z)\, \bar{\phi}_{j,k}, \quad z \in \Gamma_j,$$

$$\alpha_{\psi_j}(z) = \sum_{k=1}^{n} N_{j,k}(z)\, \bar{\psi}_{j,k}, \quad z \in \Gamma_j \tag{32}$$

where $\bar{\phi}_{j,k}$ and $\bar{\psi}_{j,k}$ are the specified nodal values at node $z_{j,k}$. For simplicity, the above function definitions can be written as

$$\alpha_{\phi_j}(z) = N_{j,k}\, \bar{\phi}_{j,k}$$

and (33)

$$\alpha_{\psi_j}(z) = N_{j,k}\, \bar{\psi}_{j,k}$$

Although it is assumed that the same basis functions be used for both $\alpha_{\phi_j}(z)$ and $\alpha_{\psi_j}(z)$, this is not required. However, the continuity definition of the basis functions is required.

Define a continuous global function $G(z)$ on Γ by

$$G(z) = \sum_{j=1}^{m} (N_{j,k}\, \bar{\phi}_{j,k} + \mathrm{i}\, N_{j,k}\, \bar{\psi}_{j,k}), \quad z \in \Gamma_j \tag{34}$$

where

$$G(z_{j,k}) = \bar{\phi}_{j,k} + \mathrm{i}\, \bar{\psi}_{j,k}.$$

An approximation function $\hat{\omega}(z)$ can be defined on $\Omega \cup \Gamma$ by

$$\hat{\omega}(z) = \frac{1}{2\pi i} \int_{\Gamma} \frac{G(\zeta)\, d\zeta}{\zeta - z}, \quad z \in \Omega, \quad z \notin \Gamma. \tag{35}$$

Because $G(z)$ is a continuous function on Γ, then $\hat{\omega}(z)$ is an analytic function in Ω. Therefore, the function $\hat{\omega}(z)$ can be split into the real and imaginary components

$$\hat{\omega}(z) = \hat{\phi}(z) + i\,\hat{\psi}(z)$$

where $\hat{\phi}(z)$ and $\hat{\psi}(z)$ are real valued functions which satisfy the Laplace equation on Ω.

If $\phi(x, y)$ and $\psi(x, y)$ are known continuously on Γ and the boundary basis functions are chosen on each Γ_j such that $G(z) = \phi(z) + i\,\psi(z)$ on Γ, then $\hat{\omega}(z) = \omega(z)$ on $\Omega \cup \Gamma$. Generally, however, $\phi(z)$ and $\psi(z)$ are known only on portions of Γ such that $\phi(z)$ is given on Γ_a and $\psi(z)$ is given on Γ_b where $\Gamma_a \cup \Gamma_b = \Gamma$. Then half of the specified nodal values are unknown on Γ. Two methods of estimating values to be used for the unknown specific nodal values are described in the following:

Case I. Suppose there are N nodal points on Γ, and N_a values of $\phi(z)$ and N_b values of $\psi(z)$ are known on Γ where $N_a + N_b = N$ and $N_a, N_b > 0$. A set of values for the unknown specified nodal values can be developed by defining the matrix system

$$\begin{Bmatrix} \bar{\phi}_1 \\ \bar{\phi}_2 \\ \vdots \\ \bar{\phi}_{N_a} \\ \bar{\psi}_{N_a+1} \\ \vdots \\ \bar{\psi}_N \end{Bmatrix} = \begin{Bmatrix} \hat{\phi}_1 \\ \hat{\phi}_2 \\ \vdots \\ \hat{\phi}_{N_a} \\ \hat{\psi}_{N_a+1} \\ \vdots \\ \hat{\psi}_N \end{Bmatrix} \tag{36}$$

where $\bar{\phi}_1$ and $\hat{\phi}_1$ indicate specified and approximation functional nodal values respectively. Solving the above matrix system will determine values for the unknown specified nodal values $\{\bar{\psi}_1, \ldots, \bar{\psi}_{N_a}, \bar{\phi}_{N_a+1}, \ldots, \bar{\phi}_N\}$.

Case II. Analogous to case I. the unknown specified nodal values can be estimated by defining

$$\begin{Bmatrix} \bar{\psi}_1 \\ \bar{\psi}_2 \\ \vdots \\ \bar{\psi}_{N_a} \\ \bar{\phi}_{N_a+1} \\ \vdots \\ \bar{\phi}_N \end{Bmatrix} = \begin{Bmatrix} \hat{\psi}_1 \\ \hat{\psi}_2 \\ \vdots \\ \hat{\psi}_{N_a} \\ \hat{\phi}_{N_a+1} \\ \vdots \\ \hat{\phi}_N \end{Bmatrix}. \tag{37}$$

This matrix system will also determine a set of values for $\{\bar{\psi}_1, \ldots, \bar{\psi}_{N_a}, \bar{\phi}_{N_a+1}, \ldots, \bar{\phi}_N\}$.

Using either set of values for the unknown specified nodal values on Γ will completely define an approximation function $\hat{\omega}(z)$ which is analytic on Ω. A property of $\hat{\omega}(z)$ is as follows:

Case I. The $\hat{\omega}(z)$ function values agree with the known specified nodal values.

Case II. The $\hat{\omega}(z)$ function values equal the estimated values for the unknown specified nodal values.

It can be seen that the Case I and Case II approximation functions differ and that a better notation for these two approximators is $\hat{\omega}_{\mathrm{I}}(z)$ and $\hat{\omega}_{\mathrm{II}}(z)$, respectively. A weighting factor $0 \leqq \eta \leqq 1$ can be introduced such that a more complete approximation function $\hat{\omega}(\eta)$ is defined by

$$\hat{\omega}(\eta) = \hat{\omega}_{\mathrm{I}}(1-\eta) + \hat{\omega}_{\mathrm{II}}(\eta). \tag{38}$$

Obviously, $\hat{\omega}(\eta)$ is also analytic on Ω.

Generally, it is preferable to use $\hat{\omega}(1)$ where all basis functions are linear polynomials on each Γ_j. Such a model utilizes m nodes and m boundary elements on Γ, and is very suitable for modeling error analysis and subsequent model refinements.

7.6 Approximation Error from the CVBEM

Let $\hat{\omega}(z)$ be an approximation function defined on $\Omega \cup \Gamma \in P$ such that

$$\hat{\omega}(z) = \frac{1}{2\pi \mathrm{i}} \int_{\Gamma} \frac{G(\zeta)\, d\zeta}{\zeta - z}; \quad z \in \Omega, \quad z \notin \Gamma$$

where $G(\zeta)$ is a continuous global trial function defined on Γ. Then $\hat{\omega}(z)$ is analytic in Ω. Let Γ^- be a simply connected contour which is a constant distance δ^* from boundary Γ such that Γ^- lies in the interior of Ω. Let $\omega(z) = \phi(z) + \mathrm{i}\,\psi(z)$ be an analytic function defined on $\Omega \cup \Gamma$ such that $\phi(z)$ and $\psi(z)$ solve the subject boundary value problem. The numerical modeling objective is to determine a $\hat{\omega}(z)$ such that for some $\varepsilon > 0$

$$|\omega(z) - \hat{\omega}(z)| < \varepsilon, \quad z \in \Gamma^-.$$

The boundary conditions which are part of the problem are assumed to be known of

$$\phi(z), \quad \text{for } z \in \Gamma_a$$

and

$$\psi(z), \quad \text{for } z \in \Gamma_b$$

where $\Gamma_a \cup \Gamma_b = \Gamma$, and Γ_a and Γ_b both have finite length. Both Γ_a and Γ_b may be composed of a finite number of line segments each of nonzero length.

In order to indicate what harmonic function $\phi(z)$ or $\psi(z)$ is known at a certain point $z \in \Gamma$, the following notation is used for $\omega(z)$:

$$\omega(z) = \Delta\xi_k + \Delta\xi_u \tag{39}$$

where the symbol Δ indicates

$$\Delta = \begin{cases} 1; & \text{if} \quad \xi_k \text{ (or } \xi_u\text{) are } \phi(z) \text{ values} \\ \mathrm{i}; & \text{if} \quad \xi_k \text{ (or } \xi_u\text{) are } \psi(z) \text{ values.} \end{cases}$$

The subscripts k and u indicate whether the nodal value is known or unknown, respectively.

For any z interior of Γ, there exists a Γ^- such that z is interior of Γ^- and

$$\omega(z) = \frac{1}{2\pi\,\mathrm{i}} \int_{\Gamma^-} \frac{\omega(\zeta)\,d\zeta}{\zeta - z}. \tag{40}$$

The approximation function $\hat{\omega}(z)$ is analytic on Ω and is therefore analytic on Γ^- and its interior, Ω^-. Then

$$\hat{\omega}(z) = \frac{1}{2\pi\,\mathrm{i}} \int_{\Gamma^-} \frac{\hat{\omega}(\zeta)\,d\zeta}{\zeta - z} + \frac{1}{2\pi\,\mathrm{i}} \int_{\Gamma} \frac{G(\zeta)\,d\zeta}{\zeta - z}. \tag{41}$$

An error function $e(z)$ is

$$e(z) = \omega(z) - \hat{\omega}(z), \quad z \in \Omega^- \cup \Gamma^-. \tag{42}$$

Then $e(z)$ is analytic on $\Omega^- \cup \Gamma^-$ and

$$\int_{\Gamma^-} e(\zeta)\,d\zeta = 0, \quad \zeta \in \Omega^- \cup \Gamma^-. \tag{43}$$

Let z_j^- be the closest point on Γ^- to $z_j \in \Gamma$. Using (39),

$$\hat{\omega}(z_j^-) = \bar{\phi}(z_j^-) + \mathrm{i}\,\hat{\psi}(z_j^-) \tag{44}$$

or

$$\hat{\omega}(z_j^-) = \Delta\hat{\xi}_k(z_j^-) + \Delta\hat{\xi}_u(z_j^-). \tag{45}$$

Then

$$e(z_j^-) = \Delta\xi_k(z_j^-) - \Delta\hat{\xi}_k(z_j^-) + \Delta\xi_u(z_j^-) - \Delta\hat{\xi}_u(z_j^-). \tag{46}$$

Equation (46) can be rewritten as

$$e(z_j^-) = \Delta\left(\xi_k(z_j^-) - \hat{\xi}_k(z_j^-)\right) + \Delta\left(\xi_u(z_j^-) - \hat{\xi}_u(z_j^-)\right)$$

where the component $\Delta\left(\xi_k(z_j^-) - \hat{\xi}_k(z_j^-)\right)$ is known from the given specified nodal values on Γ and from the $\hat{\omega}(z)$ approximation function nodal values. Thus for $\Delta\left(\xi_k(z_j^-) - \hat{\xi}_k(z_j^-)\right)$ known continuously on Γ^-,

$$\int_{\Gamma^-} \Delta\left(\xi_k(\zeta) - \hat{\xi}_k(\zeta)\right) d\zeta = \int_{\Gamma^-} \Delta\left(\hat{\xi}_u(\zeta) - \xi_u(\zeta)\right) d\zeta.$$

Let $\delta > 0$ be a constant distance between Γ and Γ^- such that $\min |z - z^-| = \delta$ for $z \in \Gamma$ and $z^- \in \Gamma^-$, then

$$\lim_{\delta \to 0} \int_{\Gamma^-} \Delta (\xi_k(\zeta) - \hat{\xi}_k(\zeta))\, d\zeta = \int_{\Gamma} \Delta (\xi_k(\zeta) - \hat{\xi}_k(\zeta))\, d\zeta \tag{47}$$

and

$$\lim_{\delta \to 0} \int_{\Gamma^-} \Delta (\hat{\xi}_u(\zeta) - \xi_u(\zeta))\, d\zeta = \int_{\Gamma} \Delta (\hat{\xi}_u(\zeta) - \xi_u(\zeta))\, d\zeta\,. \tag{48}$$

Thus an integrated error measure is determined on Γ which relates the integrated error of the unknown nodal values to the integrated error of the known nodal values,

$$\int_{\Gamma} \Delta (\xi_k(\zeta) - \hat{\xi}_k(\zeta))\, d\zeta = \int_{\Gamma} \Delta (\hat{\xi}_u(\zeta) - \xi_u(\zeta))\, d\zeta. \tag{49}$$

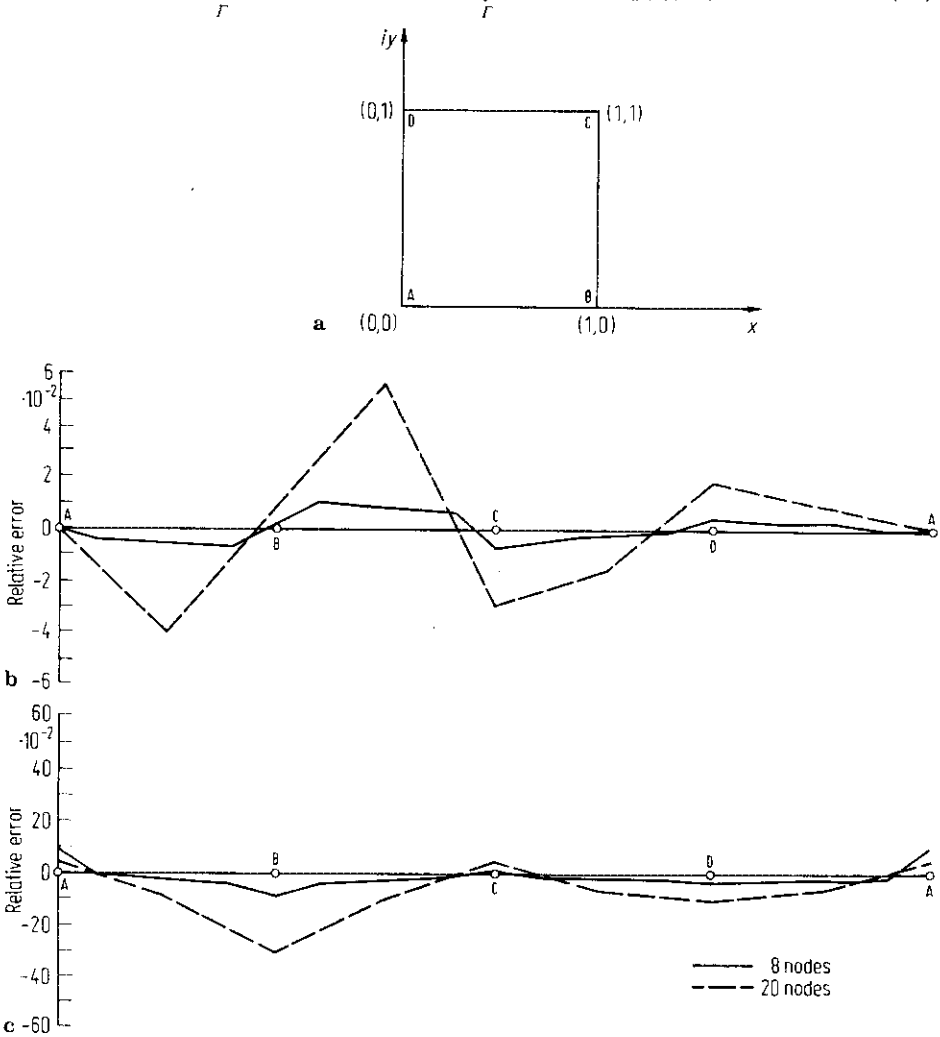

Fig. 9. **a** Problem geometry for $\omega = e^z$. **b** Plot of $\Delta (\xi_k - \hat{\xi}_k)$ fpr $\omega = e^z$ problem. **c** Plot of $\Delta (\xi_u - \hat{\xi}_u)$ for $\omega = e^z$ problem

7.7 A CVBEM Modeling Strategy to Reduce Approximation Error

In Sect. 5 the error $e(z)$ function was examined and it was concluded that an integrated error of the unknown nodal values can be calculated on Γ.

A strategy to reduce modeling error is as follows:

Step (1): Use a case II matrix system to estimate the unknown nodal variables. This system results in an approximator $\hat{\omega}(z)$ such that generally $\Delta(\xi_k(z_j) - \hat{\xi}_k(z_j)) \neq 0$.

Step (2): Using the defined approximator $\hat{\omega}(z)$, determine the $\Delta\hat{\xi}(z_j)$ values, $j = 1, 2, \ldots, m$,

Step (3): Determine $\Delta(\xi_k(z_j) - \hat{\xi}_k(z_j))$, $j = 1, 2, \ldots, m$,

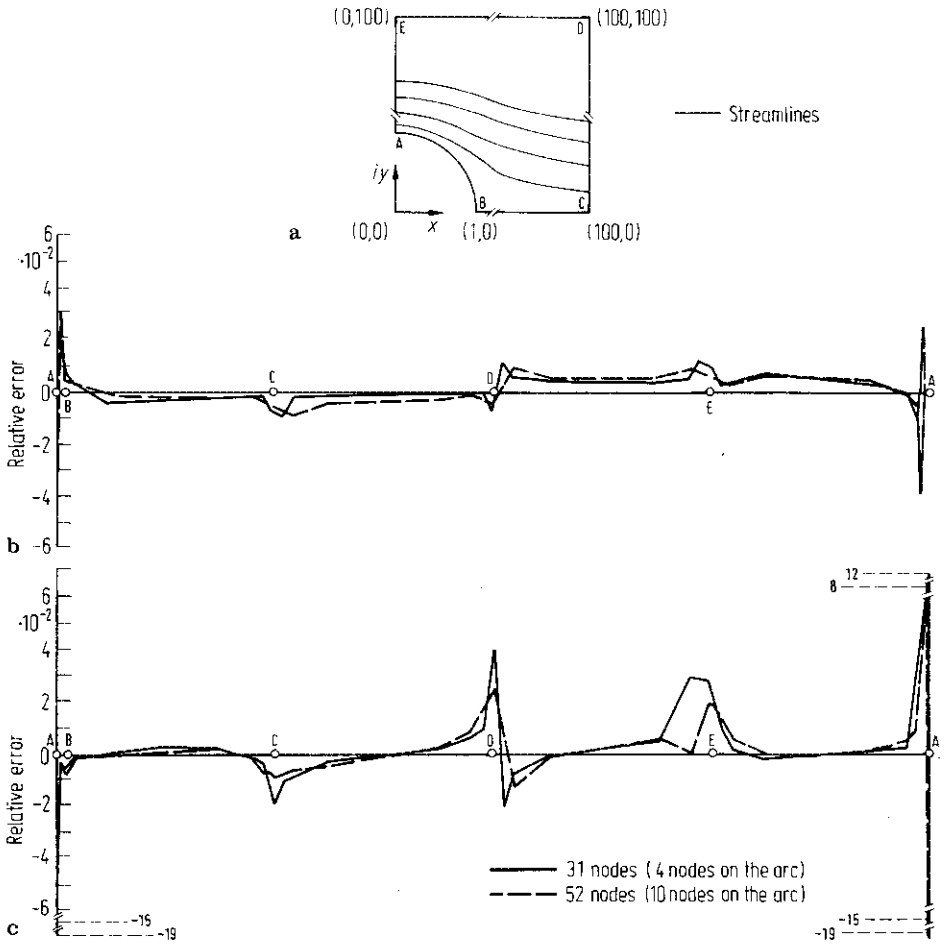

Fig. 10. **a** Problem geometry for $\omega = Z + Z^{-1}$ (ideal fluid over a cylinder). **b** Plot of $\Delta(\xi_k - \hat{\xi}_k)$ for $\omega = Z + Z^{-1}$ problem. **c** Plot of $\Delta(\xi_u - \hat{\xi}_u)$ for $\omega = Z + Z^{-1}$ problem

Step (4): Locate regions $\mathscr{S}_e$ on Γ where $\Delta(\xi_k(z_j) - \hat{\xi}(z_j))$ is large,
Step (5): Add nodal points to each $\mathscr{S}_e$,
Step (6): Return to step (1).

This modeling strategy is essentially an adaptive integration scheme which attempts to minimize $\Delta(\xi_k(z) - \hat{\xi}_k(z))$ on Γ by reducing the integration error on each $\mathscr{S}_e$ due to poor match of $G(z)$ to $\omega(z)$. To illustrate this procedure, several sample problems will be studied where the solution to the boundary value problem, $\omega(z)$, is known.

Example 2. Consider the simply connected domain

$$\Omega: \{z \mid 0 \leqq x \leqq 1, 0 \leqq y \leqq 1\}$$

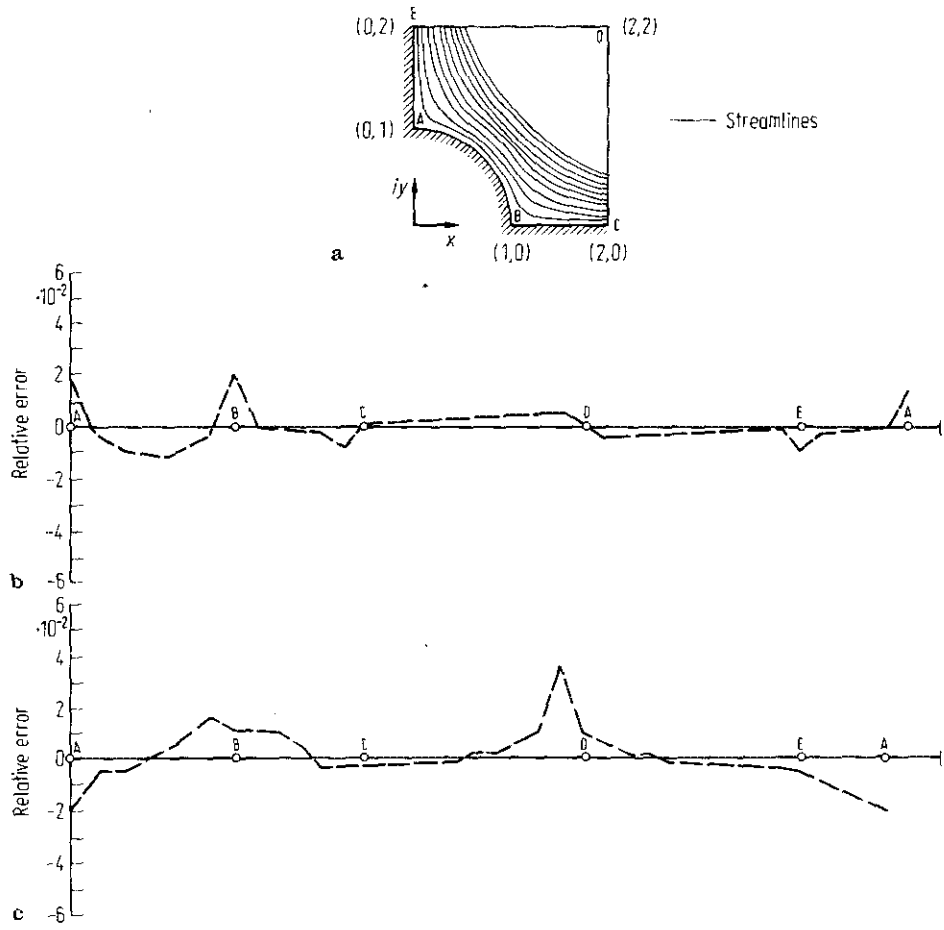

Fig. 11. **a** Problem geometry for $\omega = Z^2 + Z^{-2}$ (ideal fluid around a cylindrical corner). **b** Plot of $\Delta(\xi_k - \hat{\xi}_k)$ for $\omega = Z^2 + Z^{-2}$ problem. **c** Plot of $\Delta(\xi_u - \hat{\xi}_u)$ for $\omega = Z^2 + Z^{-2}$ problem

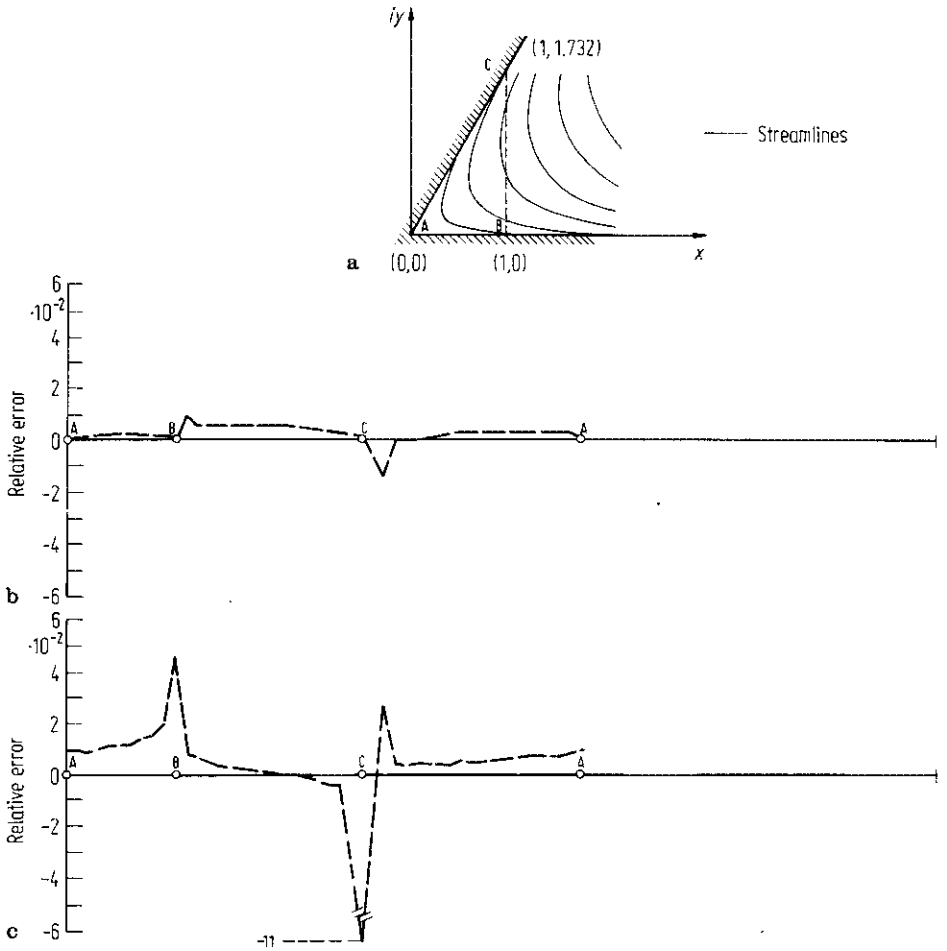

Fig. 12. **a** Problem geometry for $\omega = Z^3$ (ideal fluid around an angular region). **b** Plot of $\Delta(\xi_k - \hat{\xi}_k)$ for $\omega = Z^3$ problem. **c** Plot of $\Delta(\xi_u - \hat{\xi}_u)$ for $\omega = Z^3$ problem

and the analytic function $\omega = e^z$. Figure 9a shows the problem geometry (uniform nodal point placement). Several trials of approximation were made by adding nodal points according to Sect. 5. Figure 9b shows the relative error plots of $\Delta(\xi_k - \hat{\xi}_k)$ along Γ, and Fig. 9c shows the corresponding plot for $\Delta(\xi_u - \hat{\xi}_u)$ along Γ. From the figures, the approximation function $\hat{\omega}(z)$ better approximates $\omega(z) = e^z$ along Γ as the number of nodes are increased.

Example 3. Ideal fluid flow around a cylinder has the analytic model of $\omega(z) = A(z + z^{-1})$. Figure 10 shows the CVBEM results in modeling this problem.

Examples 4, 5, and 6. Ideal fluid flow around a cylindrical corner, around an angular region, and between a source and sink, are shown in the Figs. 11 through 13. Similar to the previous applications, plots of the known and unknown boundary condition CVBEM error distributions are shown.

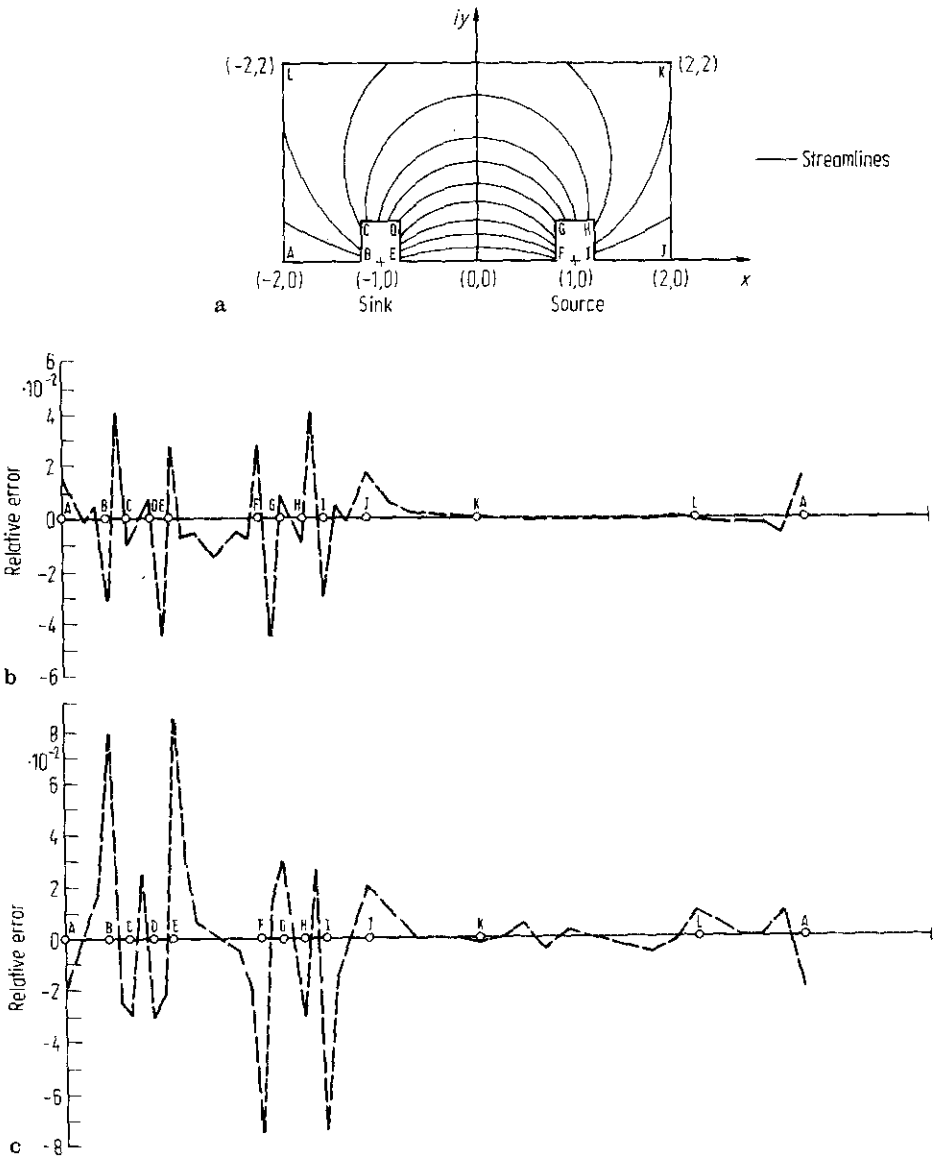

Fig. 13. **a** Problem geometry for $\omega = \log \dfrac{Z-1}{Z+1}$ (source and sink of equal strength). **b** Plot of $\Delta(\xi_k - \hat{\xi}_k)$ for $\omega = \log \dfrac{Z-1}{Z+1}$ problem. **c** Plot of $\Delta(\xi_u - \hat{\xi}_u)$ for $\omega = \log \dfrac{Z-1}{Z+1}$ problem

7.8 Expansion of the H_k Approximation Function

In this section, the CVBEM H_k approximation function $\hat{\omega}_k(z)$ will be expanded into the form

$$\hat{\omega}_k(z) = \sum_j P_j^k(z) \ln(z_j - z) + R_k(z) \tag{50}$$

where $P_j^k(z)$ is an order k complex polynomial on element Γ_j, and $R_k(z)$ is an order k reference complex polynomial. Should the solution to the boundary value problem $\omega(z)$, be an order k (or less) polynomial, then necessarily

$$\hat{\omega}_k(z) = \omega(z) = P_j^k(z). \tag{51}$$

The expansion of the H_1 and H_0 approximation functions will be developed first, with the results then generalized to the arbitrary H_k approximation function which is based on order k polynomial basis functions on each boundary element.

Let $\Omega \cup \Gamma \in P$ and $G_1(\zeta)$ be a linear global trial function. The CVBEM develops an H_1 approximation function $\hat{\omega}_1(z)$ by

$$2\pi i\, \hat{\omega}_1(z) = \sum_{j=1}^{m} \int_{\Gamma_j} \frac{G_1(\zeta)\, d\zeta}{\zeta - z} \tag{52}$$

where

$$\Gamma = \bigcup_{j=1}^{m} \Gamma_j.$$

Solving each of the boundary element integrals gives

$$2\pi i\, \hat{\omega}_1(z) = \sum_{j=1}^{m} (\bar{\omega}_{j+1} - \bar{\omega}_j) + \sum_{j=1}^{m} \left[\bar{\omega}_{j+1} \left(\frac{z - z_j}{z_{j+1} - z_j} \right) - \bar{\omega}_j \left(\frac{z - z_{j+1}}{z_{j+1} - z_j} \right) \right] h_j \tag{53}$$

where $h_j = \ln(z_{j+1} - z) - \ln(z_j - z)$, and $z \in \Omega$ but $z \notin \Gamma$.

Rewriting (53), the first summation term is zero and

$$2\pi i\, \hat{\omega}_1(z) = \sum_{j=1}^{m} \left[\bar{\omega}_{j+1} \left(\frac{z - z_j}{z_{j+1} - z_j} \right) - \bar{\omega}_j \left(\frac{z - z_{j+1}}{z_{j+1} - z_j} \right) \right] [\ln(z_{j+1} - z) - \ln(z_j - z)]. \tag{54}$$

The transcendental $\ln(z_j - z)$ function is multivalued with the principal value assumed given by

$$\ln(z_j - z) = \ln |z_j - z| + i \arg(z_j - z) \tag{55}$$

where $0 \leqq \arg(z_j - z) < 2\pi$, and $z_j \neq z$. Thus point $z \in \Omega$ is a branch point of the $\ln(z_j - z)$ function. For convenience, let the branch cut on $\ln(z_j - z)$ pass from point z through nodal point $z_1 \in \Gamma$. Then as the boundary integral on Γ is solved in the positive sense, it is noted that in the evaluation of the h_j terms,

$$\ln(z_1 - z) = \begin{cases} \ln |z_1 - z|, & \text{when evaluating the integral on element } \Gamma_1 \\ \ln |z_1 - z| + 2\pi i, & \text{when evaluating the integral on element } \Gamma_m \end{cases} \tag{56}$$

Using the results of (56), Eq. (54) can be written as

$$2\pi i\,\hat{\omega}_1(z) = -\left[\bar{\omega}_2\left(\frac{z-z_1}{z_2-z_1}\right) - \bar{\omega}_1\left(\frac{z-z_2}{z_2-z_1}\right)\right]\ln(z_1-z)$$

$$+\sum_{j=2}^{m}\left[-\bar{\omega}_{j+1}\left(\frac{z-z_j}{z_{j+1}-z_j}\right) + \bar{\omega}_j\left(\frac{z-z_{j+1}}{z_{j+1}-z_j}\right)\right.$$

$$\left.+\,\bar{\omega}_j\left(\frac{z-z_{j-1}}{z_j-z_{j-1}}\right) - \bar{\omega}_{j-1}\left(\frac{z-z_j}{z_j-z_{j-1}}\right)\right]\ln(z_j-z)$$

$$+\left[\bar{\omega}_1\left(\frac{z-z_m}{z_1-z_m}\right) - \bar{\omega}_m\left(\frac{z-z_1}{z_1-z_m}\right)\right][\ln(z_1-z)+2\pi i]. \tag{57}$$

In (57), the $2\pi i$ is added to the $\ln(z_1-z)$ term due to the complete circuit on Γ around branch point z. The above expansion is simplified by noting

$$\bar{\omega}_j\left(\frac{z-z_{j-1}}{z_j-z_{j-1}}\right) = \bar{\omega}_j\left(\frac{z-z_j}{z_j-z_{j-1}}\right) + \bar{\omega}_j \tag{58}$$

and

$$\bar{\omega}_j\left(\frac{z-z_{j+1}}{z_{j+1}-z_j}\right) = \bar{\omega}_j\left(\frac{z-z_j}{z_{j+1}-z_j}\right) - \bar{\omega}_j. \tag{59}$$

Substituting (58) and (59) into (57) and combining terms,

$$2\pi i\,\hat{\omega}_1(z) = \left[\sum_{j=2}^{m}\left[\left(\frac{\bar{\omega}_j-\bar{\omega}_{j-1}}{z_j-z_{j-1}}\right) - \left(\frac{\bar{\omega}_{j+1}-\bar{\omega}_j}{z_{j+1}-z_j}\right)\right](z-z_j)\ln(z_j-z)\right]$$

$$-\left[\bar{\omega}_2\left(\frac{z-z_1}{z_2-z_1}\right) - \bar{\omega}_1\left(\frac{z-z_1}{z_2-z_1}\right) + \bar{\omega}_1\right]\ln(z_1-z)$$

$$+\left[\bar{\omega}_1\left(\frac{z-z_1}{z-z_m}\right) + \bar{\omega}_1 - \bar{\omega}_m\left(\frac{z-z_1}{z_1-z_m}\right)\right][\ln(z_1-z)+2\pi i]. \tag{60}$$

Rearranging (60) gives the final form of the expansion

$$2\pi i\,\hat{\omega}_1(z) = \left[\sum_{j=1}^{m}\left[\left(\frac{\bar{\omega}_j-\bar{\omega}_{j-1}}{z_j-z_{j-1}}\right) - \left(\frac{\bar{\omega}_{j+1}-\bar{\omega}_j}{z_{j+1}-z_j}\right)\right](z-z_j)\ln(z_j-z)\right]$$

$$+2\pi i\left[\bar{\omega}_1 + \left(\frac{\bar{\omega}_1-\bar{\omega}_m}{z_1-z_m}\right)(z-z_1)\right]. \tag{61}$$

Thus, the H_1 approximation function can be written as the sum

$$\hat{\omega}_1(z) = \sum_{j=1}^{m}\gamma_j(z_j-z)\ln(z_j-z) + R_1(z) \tag{62}$$

where the γ_j are complex constants defined by

$$\gamma_j = \frac{1}{2\pi i}\left[\left(\frac{\bar{\omega}_{j+1} - \bar{\omega}_j}{z_{j+1} - z_j}\right) - \left(\frac{\bar{\omega}_j - \bar{\omega}_{j-1}}{z_j - z_{j-1}}\right)\right] \tag{63}$$

and $R_1(z)$ is a reference polynomial (of order 1) given by

$$R_1(z) = \bar{\omega}_1 + \left(\frac{\bar{\omega}_1 - \bar{\omega}_m}{z_1 - z_m}\right)(z - z_1). \tag{64}$$

From the expansion of (62), it is easily shown that the limiting value of $\hat{\omega}_1(z)$ exists as z approaches node z_i

$$\lim_{z \to z_i} \hat{\omega}_1(z) = \left[\sum_{\substack{j=1 \\ j \neq i}}^{m} \gamma_j (z_j - z_i) \ln (z_j - z_i)\right] + R_1(z_i) \tag{65}$$

where for $j = i$ in (65)

$$\lim_{z \to z_i} \gamma_i (z_i - z) \ln (z_i - z) = 0. \tag{66}$$

Additionally, should $\omega(z)$ be a linear (or constant) polynomial on $\Omega \cup \Gamma$, then $\hat{\omega}(z)$ is exactly equal to $\omega(z)$.

In a similar fashion, the H_0 approximation function can be expanded as (for appropriate branches of the logarithm)

$$2\pi i\, \hat{\omega}_0(z) = \sum_{j=1}^{m} \bar{\omega}_j \ln\left(\frac{z_{j+1} - z}{z_j - z}\right) \tag{67}$$

where again $\bar{\omega}_{m+1} \equiv \bar{\omega}_1$, $z_{m+1} \equiv z_1$. Rewriting (67),

$$\begin{aligned} 2\pi i\, \hat{\omega}_0(z) = {} & \bar{\omega}_1 \ln (z_2 - z) - \bar{\omega}_1 \ln (z_1 - z) + \bar{\omega}_2 \ln (z_3 - z) \\ & - \bar{\omega}_2 \ln (z_2 - z) + \ldots + \bar{\omega}_m [\ln (z_1 - z) + 2\pi i] - \bar{\omega}_m \ln (z_m - z). \end{aligned} \tag{68}$$

Thus using the notation that $\bar{\omega}_0 \equiv \bar{\omega}_m$,

$$2\pi i\, \hat{\omega}_0(z) = \left[\sum_{j=1}^{m} (\bar{\omega}_{j-1} - \bar{\omega}_j) \ln (z_j - z)\right] + 2\pi i\, \bar{\omega}_m \tag{69}$$

or in the form of (62),

$$\hat{\omega}_0(z) = \left[\sum_{j=1}^{m} \gamma_j \ln (z_j - z)\right] + R_0(z) \tag{70}$$

where in this case

$$\gamma_j = \frac{-1}{2\pi i}(\bar{\omega}_j - \bar{\omega}_{j-1}) \tag{71}$$

and

$$R_0(z) = \bar{\omega}_m. \tag{72}$$

The above procedure can be extended to the H_k approximation function $\hat{\omega}_k(z)$. Let Γ be discretized into m $(k+1)$-node boundary elements, and assume that order k polynomial basis functions are used on each element Γ_j. Thus on Γ_j, the order k global trial function is

$$G_k(\zeta) = \sum_{j=1}^{k+1} N_{j,i}\,\bar{\omega}_{j,i}, \quad \zeta \in \Gamma_j. \tag{73}$$

The $\hat{\omega}_k(z)$ approximation function is

$$2\pi i\,\hat{\omega}_k(z) = \sum_{j=1}^{m} \int_{\Gamma_j} \frac{G_k(\zeta)\,d\zeta}{\zeta - z}, \quad z \in \Omega,\ z \notin \Gamma. \tag{74}$$

The contribution to (74) from Γ_j is determined by

$$\int_{\Gamma_j} \frac{G_k(\zeta)\,d\zeta}{\zeta - z} = \sum_{j=1}^{k+1} \bar{\omega}_{j,i} \int_{\Gamma_j} \frac{N_{j,i}(\zeta)\,d\zeta}{\zeta - z}. \tag{75}$$

But each polynomial basis function is of the form

$$N_{j,i}(\zeta) = \begin{cases} a_{i,0} + a_{i,1}\zeta + \ldots + a_{i,k}\zeta^k, & \zeta \in \Gamma_j \\ 0, & \zeta \notin \Gamma_j \end{cases} \tag{76}$$

and for $z \in \Gamma_j$

$$N_{j,i}(z) = \begin{cases} 1, & z = z_{j,i} \\ 0, & z = z_{j,n}, \quad n \neq i. \end{cases} \tag{77}$$

Thus

$$\int_{\Gamma_j} \frac{N_{j,i}(\zeta)\,d\zeta}{\zeta - z} = \int_{\Gamma_j} \frac{(a_{i,0} + a_{i,1}\zeta + \ldots + a_{i,k}\zeta^k)\,d\zeta}{\zeta - z} \tag{78}$$

$$= \int_{\Gamma_j} [a_{i,k}\zeta^{k-1} + (z\,a_{i,k} + a_{i,k-1})\zeta^{k-2} + \ldots + (z^{k-1}a_{i,k} + \ldots + a_{i,1})]\,d\zeta$$
$$+ (z^k a_{i,k} + z^{k-1}a_{i,k-1} + \ldots + z\,a_{i,1} + a_{i,0}) \int_{\Gamma_j} \frac{d\zeta}{\zeta - z}. \tag{79}$$

The complex integral is evaluated by

$$(a_{i,k}z^k + \ldots + a_{i,1}z + a_{i,0}) \int_{\Gamma_j} \frac{d\zeta}{\zeta - z} = (a_{i,k}z^k + \ldots + a_{i,0}) \ln\left(\frac{z_{j,k+1} - z}{z_{j,1} - z}\right). \tag{80}$$

Comparing (80) to the results of the H_1 and H_0 approximation, function $\hat{\omega}_k(z)$ can be expanded into the form

$$\hat{\omega}_k(z) = \sum_{j=1}^{m} P_j^k(z) \ln(z_j - z) + R_k(z) \tag{81}$$

where $P_j^k(z)$ is an order k complex polynomial defined on element Γ_j, and $R_k(z)$ is a reference polynomial of order k which occurs due to the circuit on Γ about branch point z of the function $\ln(z_j - z)$.

7.9 Upper Half Plane Boundary Value Problems

Further insight into the CVBEM is gained by examining the approximation accuracy in modeling Dirichlet boundary value problems in the upper half plane. In this section, the Dirichlet problem is studied where $\psi(z)$ is known continuously on boundary Γ and a single reference value of $\phi(z)$ is known. The Dirichlet problem of $\phi(z)$ known on Γ is analogous to the above case due to $f(z) = \mathrm{i}\,\omega(z)$ being an analytic function (in which case $f(z) = -\psi(z) + \mathrm{i}\,\phi(z)$, and $\phi(z)$ is therefore the stream function of $f(z) = \mathrm{i}\,\omega(z)$).

By assumption Γ is a simple closed polygon. The Schwarz-Christoffel transformation $T(z)$ maps Γ onto the real axis ($-\infty < x < \infty$), and domain Ω onto the upper half-plane ($y > 0$). The transformation is

$$T(z) = A \int (z - x_1)^{\alpha_1/\pi - 1} \ldots (z - x_n)^{\alpha_n/\pi - 1}\, dz + B \tag{82}$$

where the α_i are angles (Fig. 14); A and B are constants.

Let Γ be discretized into m 2-node boundary elements Γ_j, $j = 1, 2, \ldots, m$. Then the real axis is also discretized into m boundary elements with one element, say Γ_i, being mapped by $T(z)$ into an infinite length boundary element on the real axis, Γ_i' (see Fig. 14). Assume the transformed boundary conditions on the real axis are linear distributions of $\psi'(z)$ on each Γ_i' except on Γ_i', where $\psi'(z)$ is a constant value. (All complex variables are denoted by prime to represent the transformed result.) Figure 15 shows the assumed boundary condition definition on Γ'.

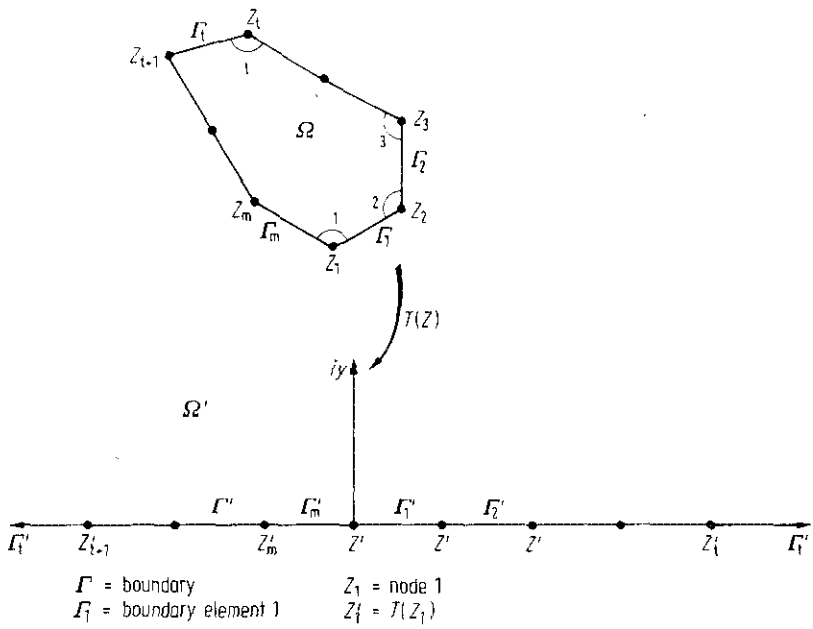

Fig. 14. Mapping of polygon Γ onto real axis by $T(Z)$ transformation

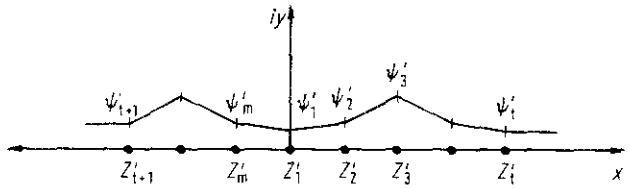

Fig. 15. Transformed boundary conditions on Γ'

For the case of $\psi'_t = \psi'_{t+1} = 0$, the solution of the boundary value problem is

$$\omega(z) = \sum_{j=1}^{m} (A_j + B_j z) \ln(z - z_j) + Cz + D, \quad z \in \Omega \cup \Gamma' \tag{83}$$

where the A_j, B_j and C, D are complex constants which have the form of the expanded H_1 approximation function $\hat{\omega}_1(z)$.

To use (83), let

$$\ln(z - z_j) = \ln R_j + \mathrm{i}\,\theta_j, \quad 0 \leqq \theta \leqq \pi, \quad R_j > 0 \tag{84}$$

where R_j and θ_j are defined in Fig. 16.

Then for every node z_j

$$(A_j + B_j z)(\ln R_j + \mathrm{i}\,\theta_j) = [(A_j + B_j x) \ln R_j - B_j y\,\theta_j] + \mathrm{i}\,[B_j y \ln R_j + (A_j + B_j x)\,\theta_j]. \tag{85}$$

On the real axis, y is identically zero and therefore for $x \neq x_j$, $j = 1, 2, \ldots, m$

$$\psi'(x, y = 0) = \sum_{j=1}^{m} (A_j + B_j x)\,\theta_j + \mathrm{Im}(Cz + D)$$

$$\phi'(x, y = 0) = \sum_{j=1}^{m} (A_j + B_j x) \ln R_j + \mathrm{Re}(Cz + D) \tag{86}$$

where on the real axis, $\theta_j = 0$ or π.

On each Γ_j, let the boundary conditions be of the form $\psi'(z \in \Gamma_j, y = 0) = a_j + b_j x$. Substituting the boundary conditions into (86) gives the matrix system

$$\left.\begin{aligned} 0 = a_1 &= \pi(A_1 + A_2 + \ldots + A_m) \\ 0 = b_1 &= \pi(B_1 + B_2 + \ldots + B_m) \end{aligned}\right\} \quad x < x'_{t+1}$$

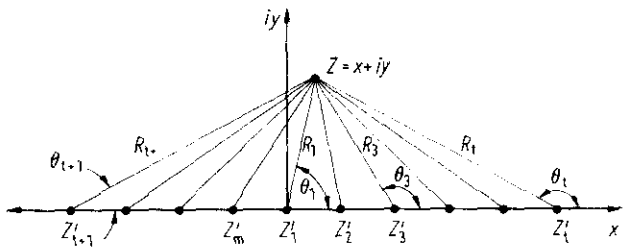

Fig. 16. Upper half plane Dirichlet problem geometry

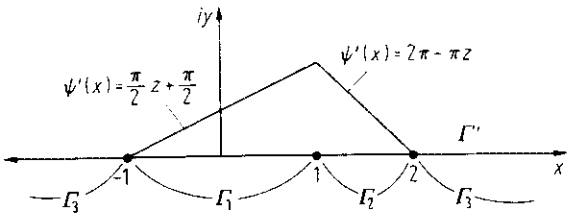

Fig. 17. Example 7 boundary conditions

$$\left.\begin{aligned} a_2 &= \pi(A_2 + \ldots + A_m) \\ &\vdots \\ b_2 &= \pi(B_2 + \ldots + B_m) \end{aligned}\right\} \quad x'_{l+1} < x < x'_{l+2}$$

$$\left.\begin{aligned} a_m &= \pi A_m \\ b_m &= \pi B_m \end{aligned}\right\} \quad x'_{l-1} < x < x'_l$$

Example 7. Let $\psi'(x)$ be given on a 3-element discretization of Γ' by (Fig. 17)

$$\psi'(x) = \begin{cases} 0, & x < -1 \\ \frac{\pi}{2} x + \frac{\pi}{2}, & -1 \leqq x \leqq 1 \\ 2\pi - \pi x, & 1 \leqq x \leqq 2 \\ 0, & x \geqq 2 \end{cases}$$

Then $a_2 = \frac{\pi}{2}$, $b_2 = \frac{\pi}{2}$; $a_3 = 2\pi$, $b_3 = -\pi$. Using the relations given in (86), $m = 3$, and

$$A_2 = a_3/\pi = 2\pi/\pi = 2$$

$$B_3 = -\pi/\pi = -1 .$$

Likewise,

$$A_2 = -1.5, \quad B_2 = 1.5; \quad A_1 = -0.5, \quad B_1 = -0.5$$

and the solution to this boundary value problem is

$$\omega(z) = (-0.5 - 0.5z)\ln(z+1) + (-1.5 + 1.5z)\ln(z-1) + (2-z)\ln(z-2),$$

for $x \neq -1, 2$ and $y \geqq 0$.

It can be noted that the solution $\omega(z)$ is of a form analogous to the H_1 approximation function expansion of Eq.(62).

7.10 The Approximate Boundary for Error Analysis

The CVBEM is used to develop an analytic approximation function $\hat{\omega}(z)$ which exactly satisfies the Laplace equation throughout the interior of the problem domain, Ω. As the values of $\hat{\omega}(z)$ approach the values of the exact solution of the boundary value problem $\omega(z)$ for all points z on the problem boundary Γ, then the

error $|\hat{\omega}(z) - \omega(z)$ is reduced throughout $\Omega \cup \Gamma$. By the Maximum Modulus Theorem, the maximum value of $|\hat{\omega}(z) - \omega(z)|$ necessarily occurs for z on Γ. One approach to reduce error is to use $|\hat{\omega}(z) - \omega(z)$ to locate additional nodal points z_j on Γ such that the global interpolation function is better adapted to fit the boundary conditions of the problem. In this fashion, the approximation function $\hat{\omega}(z)$ converges to the true solution $\omega(z)$ in a fashion analogous to an adaptive integration approach.

Rather than examining the above error values on the boundary, Γ, it is useful to determine an approximate boundary $\hat{\Gamma}$ upon which $\hat{\omega}(z)$ satisfies the given boundary conditions for $\omega(z)$ on $\hat{\Gamma}$. That is, given an approximator $\hat{\omega}(z)$, level curves of constant ϕ or ψ on Γ (where $\omega(z) = \phi + i\,\psi$ and $\hat{\omega}(z) = \hat{\phi} + i\,\hat{\psi}$) are compared to level curves of constant $\hat{\phi}$ or $\hat{\psi}$ on $\hat{\Gamma}$ where $\hat{\Gamma}$ is determined by setting the known $\phi = \hat{\phi}$ and $\psi = \hat{\psi}$. The resulting boundary $\hat{\Gamma}$ has the property that $\hat{\omega}(z)$ satisfies the specified boundary conditions on $\hat{\Gamma}$, and $\hat{\omega}(z)$ satisfies the governing Laplace equation in the interior, $\hat{\Omega}$. Consequently, $\hat{\omega}(z)$ is the exact solution to the boundary value problem with the true boundary Γ transformed into the approximate boundary $\hat{\Gamma}$.

The utilization of the approximate boundary provides the following features:

1. An exact solution of the subjection boundary value problem is provided for a transformation of the problem boundary (the complex variable transformation is undetermined).
2. The approximate boundary can be visually compared to the true boundary as to closeness of geometric fit.
3. Nodal points can be added to Γ to determine a more refined approximation $\hat{\omega}(z)$ so that $\hat{\Gamma}$ is geometrically closer to Γ in regions of high discrepancy.
4. The engineer works with a displacement of the problem boundary rather than examining a more abstract relative error propagation along the boundary.
5. The approximate boundary provides a direct visual representation of the sensitivity of the approximation $\hat{\omega}(z)$ in accommodation boundary conditions, variations in the Γ geometry, and the addition of nodal points.

In the following, several mixed boundary value problems of the Laplace equation are approximated by the CVBEM. The problems utilize boundaries Γ which geometrically coincide with lines of constant ϕ or ψ of $\omega(z)$. After developing a $\hat{\omega}(z)$, the approximate boundary $\hat{\Gamma}$ is determined by plotting the corresponding lines of constant $\hat{\phi} = \phi$ and $\hat{\psi} = \psi$ from $\hat{\omega}(z)$. In the accompanying figures, both Γ and the associated $\hat{\Gamma}$ are plotted so that a direct comparison is seen. Intuitively, as $|\hat{\Gamma} - \Gamma|$ becomes small then necessarily $|\hat{\omega}(z) - \omega(z)$ is reduced and $|\hat{\Gamma} - \Gamma| = 0$ implies $\hat{\omega}(z) = \omega(z)$.

A difficulty in using the $\hat{\omega}(z)$ function of (52) is that $\hat{\omega}(z) = 0$ for z exterior of $\Omega \cup \Gamma$. Thus an analytic continuation of $\hat{\omega}(z)$ to the exterior of $\Omega \cup \Gamma$ is needed in order to determine $\hat{\Gamma}$. One procedure to develop this analytic continuation is to use the finite series expansion of (62) modified to have the angle of the form $\arg(z_j - z)$ to be measured with respect to branch cuts originating from each nodal point and extending outwards away from $\Omega \cup \Gamma$. Figure 18 illustrates the branch cut definition needed. In this fashion, the analytical continuation of $\hat{\omega}(z)$ is available everywhere except across each branch cut.

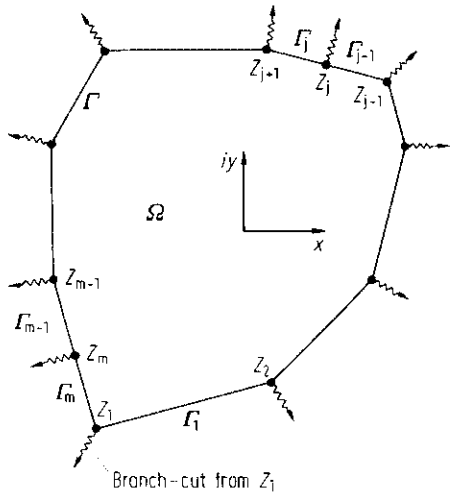

Fig. 18. The analytic continuation of $\hat{\omega}(z)$ to the exterior of $\Omega \cup \Gamma$. Note branch cuts along Γ at nodes z_j

The approximate boundary is developed by the following steps:

1. Use $\hat{\omega}(z)$ to estimate nodal values for the unknown nodal point state variable or stream function values, $\Delta\xi_U(z_j)$.
2. Using the analytic continuation of $\hat{\omega}(z)$ given by (62), determine constants γ_j by forcing $\hat{\omega}(z_j) = \Delta\xi_k(z_j) + \Delta\xi_U(z_j)$. In calculating the γ_j values, use branch cuts which lie exterior of $\Omega \cup \Gamma$ such as shown in Fig. 18.
3. Determine the approximate boundary $\hat{\Gamma}$ by locating (x, y) coordinates where level curves of $\hat{\omega}(z)$ match the boundary condition values. Because $\hat{\omega}(z_j)$ is now determined using $\Delta\xi_k(z_j)$ values, $\hat{\Gamma}$ necessarily intersects Γ at each nodal point location on Γ.

Example 7. This problem approximates the classic problem of ideal fluid flow over a cylinder. The exact solution is known to be $\omega(z) = z + 1/z$. The problem boundary Γ is specified to be the upper right quadrant as shown in the figure. Using a 47-node discretization, a $\hat{\omega}(z)$ approximator is developed. The corresponding approximate boundary $\hat{\Gamma}$ is plotted along with the true boundary Γ in Fig. 19.

Example 7 demonstrates the utility of determining an approximate boundary corresponding to CVBEM approximation functions. The approximate boundary $\hat{\Gamma}$ is developed by plotting the level curves of constant potential (or stream function) which match the boundary condition values on the problem boundary Γ. Consequently, this technique is directly applicable only to boundary value problems which have level curves for boundary conditions.

The error of approximation is manifested by the departure of the approximate boundary from the problem true boundary. Where large spatial discrepancies are observed, additional nodal points are needed to increase the approximation accuracy. The approximate boundary can often be argued to better represent the

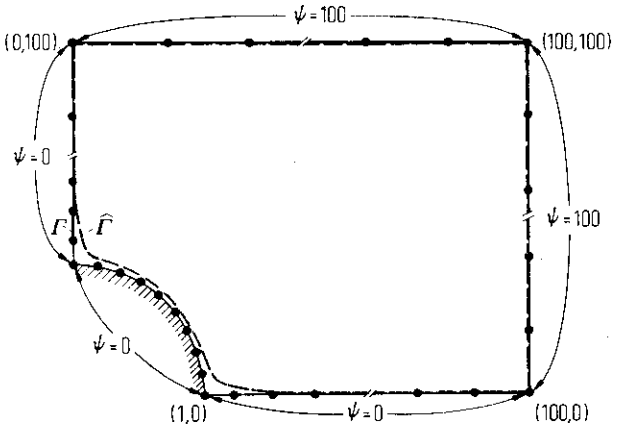

Fig. 19. Modeling ideal fluid flow over a cylinder

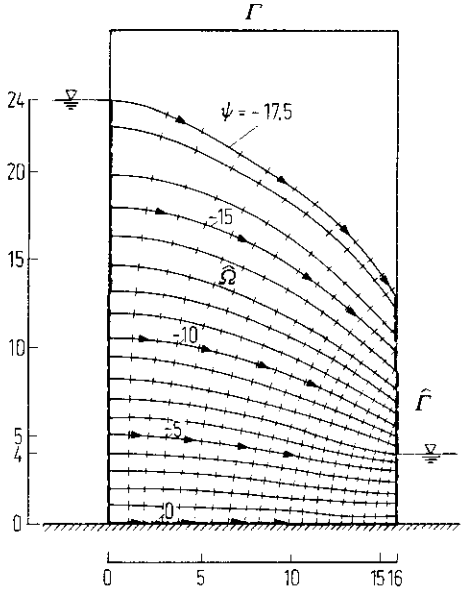

Fig. 20. Plot of streamlines and potentials for soil-water flow through a homogeneous soil

"as-built" or a more realistic problem boundary than the defined problem boundary. This latter idea is especially valid in large scale civil engineering studies where angle points are generally constructed as grossly rounded edges.

To illustrate the CVBEM approximation results within the interior of the problem domain, Figs. 20 and 21 show groundwater seepage problems with the approximate boundary, and several streamlines and lines of the constant potential plotted. Because the maximum error magnitude ε must occur on the boundary, interior values of $\hat{\omega}(z)$ necessarily differ from $\omega(z)$ in magnitude by less than ε.

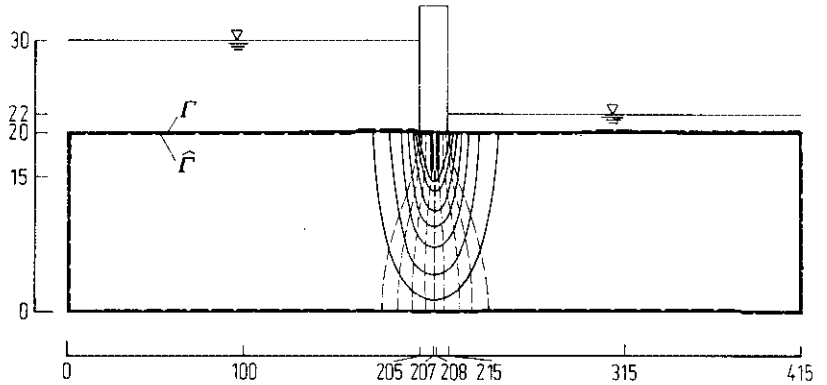

Fig. 21. Plot of streamlines and potentials for soil-water flow beneath a dam. (Note that the vertical and horizontal scales differ)

7.11 Locating Additional Nodal Points on Γ

The success of the CVBEM in developing solutions to the boundary value problem depends upon the accuracy of the trial function assumptions. Accuracy is improved by the addition of nodal points on Γ due to the subsequent reduction in the error of the trial function approximation.

The CVBEM offers a highly useful error analysis capability by simply examining the success of the CVBEM approximator in matching the boundary conditions. The usual approach to reduing error is to add nodal points on Γ where the CVBEM approximator performs poorly in meeting the specified boundary condition values.

In this section, four methods of examining CVBEM approximation error are compared as to their effectiveness in developing better $\hat{\omega}(z)$ functions by indicating where additional nodes should be added to Γ.

Method 1. A plot of relative error in matching boundary conditions continuously on Γ is obtained by subtracting the approximator function values (along Γ) from the known boundary condition values. Since only one of the conjugate functions (ϕ or ψ) is known as a boundary condition at a point, this error plot is a representation of the mixed boundary condition fit. From Sect. 4 it is noted that the unknown nodal point values can be estimated using a class I or class II CVBEM matrix system. If the class I system is used, further computation effort is needed due to this type of relative error being zero at nodal points. Thus, interior values of $\hat{\omega}(z)$ are computed on each Γ_j. If the class II system is used, this error is usually nonzero at nodal points, and is readily evaluated. After the determination of the error plot, additional nodal points are located where there is large error. Should the error be zero on each Γ_j, then $\hat{\omega}(z)$ satisfies the Laplace equation and also the prescribed boundary conditions, and $\hat{\omega}(z)$ is the exact solution.

Method 2. Generally, the prescribed boundary conditions are values of constant ϕ or ψ on each Γ_j. These values corresponds to level curves of the analytic function

$\omega(z) = \phi + i\,\psi$. After determining a $\hat{\omega}(z)$, it is convenient to determine an approximate boundary $\hat{\Gamma}$ which corresponds to the prescribed boundary conditions. From Sect. 9 an analytic continuation of $\hat{\omega}(z)$ is determined which forces $\hat{\Gamma}$ to intersect Γ at each nodal point. The resulting contour $\hat{\Gamma}$ is a visual representation of approximation error, and $\hat{\Gamma}$ coincident with Γ implies $\hat{\omega}(z) = \omega(z)$. Additional collocation points are located at regions where $\hat{\Gamma}$ deviates substantially from Γ.

Implementation on a computer is direct although considerable computation effort is required. One strategy for using this technique is to subdivide each Γ_j with several internal points (about 4 to 6) and determine $\hat{\omega}(z)$ at each point. Next, $\hat{\Gamma}$ is estimated by locating where $\hat{\omega}(z)$ matches the prescribed local boundary condition. Thus, several evaluations of $\hat{\omega}(z)$ are needed to locate a single point on $\hat{\Gamma}$. The end product, however, is very useful since it can be argued that $\hat{\omega}(z)$ is the exact solution to the boundary value problem with Γ transformed to $\hat{\Gamma}$. Thus $\hat{\Gamma}$ is a visual indication of approximation error.

Method 3. This technique includes features from both Methods 1 and 2, and yet involves a significant reduction in computer effort over Method 2 alone. First, the error distribution of Method 1 is determined along Γ between the known function (ϕ or ψ) of $\omega(z)$ and the corresponding approximation of $\hat{\omega}(z)$. The next step is to weight the error determined above (designated as $e(z)$ for $z \in \Gamma$) by the tangential gradient of the function conjugate to the local boundary condition variable. For example, if ϕ is known on Γ_n, then for $z \in \Gamma_n$ we have $e(z) = \phi - \hat{\phi}$. This relative error is weighted by $\partial\hat{\psi}/\partial s$ which is determined directly by finite differences of $\hat{\omega}(z)$. Using the Cauchy-Riemann relations, an estimated distance of departure $d(\hat{\Gamma}, \Gamma, z)$ between the approximate boundary $\hat{\Gamma}$ and the problem boundary Γ at point $z \in \Gamma$ is given by

$$d(\hat{\Gamma}, \Gamma, z) \cong \left| e_\phi(z) \Big/ \frac{\partial\hat{\psi}}{\partial s} \right|. \tag{87}$$

In (87) the error $e_\phi(z)$ has a subscript notation for the ϕ function. A similar relationship holds for the $e_\psi(z)$ error

$$d(\hat{\Gamma}, \Gamma, z) \cong \left| e_\psi(z) \Big/ \frac{\partial\hat{\phi}}{\partial s} \right|.$$

The final form of error used, $V(z)$, is the ratio

$$V(z) = \begin{cases} e_\phi^2(z) \Big/ \left| \dfrac{\partial\hat{\psi}}{\partial s} \right|, & \text{if } \phi \text{ is known at } z \\ e_\psi^2(z) \Big/ \left| \dfrac{\partial\hat{\phi}}{\partial s} \right|, & \text{if } \psi \text{ is known at } z\,. \end{cases} \tag{88}$$

Additional nodal points are defined at locations on Γ where $V(z)$ is large.

An advantage of Method 3 over Method 1 is that more weight is given to the error which also has a large distance of departure between Γ and $\hat{\Gamma}$. Similarly, Method 3 provides an improved definition of the error associated with the

approximate boundary of Method 2 by including the description of whether $e(z)$ is large or small and $\hat{\Gamma}$ has a large departure from Γ simply due to a small normal gradient of the specified boundary condition variable. Figure 22 illustrates a geometric interpretation of $V(z)$ as a "point area of error" in the CVBEM approximation. From the figure, the positive area at point z_0 equals one-half of the quantity defined in the relations of (88). Also shown in the figure is the actual approximation value $\hat{\phi}(n)$ as a function of normal distance (n) from point $z_0 \in \Gamma$.

Method 4. Because $G(\zeta)$ is continuous on Γ, $\hat{\omega}(z)$ is analytic in Ω. Thus for $z \in \Omega$ and $z \notin \Gamma$

$$\hat{\omega}(z) = \frac{1}{2\pi i} \int_{\Gamma} \frac{G(\zeta)\, d\zeta}{\zeta - z} = \frac{1}{2\pi i} \int_{\Gamma} \frac{\hat{\omega}(\zeta)\, d\zeta}{\zeta - z}. \tag{89}$$

But for $z_0 \in \Gamma$, the limit as $z \to \Gamma$ (where $z \in \Omega$) can be determined and an error $E(z_0)$ is defined by

$$E(z_0) = \lim_{z \to z_0} \frac{1}{2\pi i} \int_{\Gamma} \frac{G(z_0)\, d\zeta}{\zeta - z_0} - \frac{1}{2\pi i} \int_{\Gamma} \frac{\hat{\omega}(\zeta)\, d\zeta}{\zeta - z_0} \tag{90}$$

or simply

$$E(z_0) = \lim_{z \to z_0} \frac{1}{2\pi i} \int_{\Gamma} \frac{[G(z_0) - \hat{\omega}(\zeta)]\, d\zeta}{\zeta - z_0}. \tag{91}$$

Setting $E(z_j) = 0$ for $j = 1, 2, \ldots, m$ determines a class I or II system of equations which are used to estimate values for the unknown nodal variable function. The objective in this method is to obtain a global trial function such that in the limit $G(z_0) = \hat{\omega}(z_0)$ for all $z_0 \in \Gamma$. Thus additional nodal points are located on Γ where $G(z_0) - \hat{\omega}(z_0)$ is a maximum.

A comparison of Method 4 to Method 1 indicates that Method 4 involves approximately the same computational effort as Method 1, yet includes an error contribution for both the potential and stream functions. Thus a total error magnitude is provided by this technique which is not immediately available by the other three approaches.

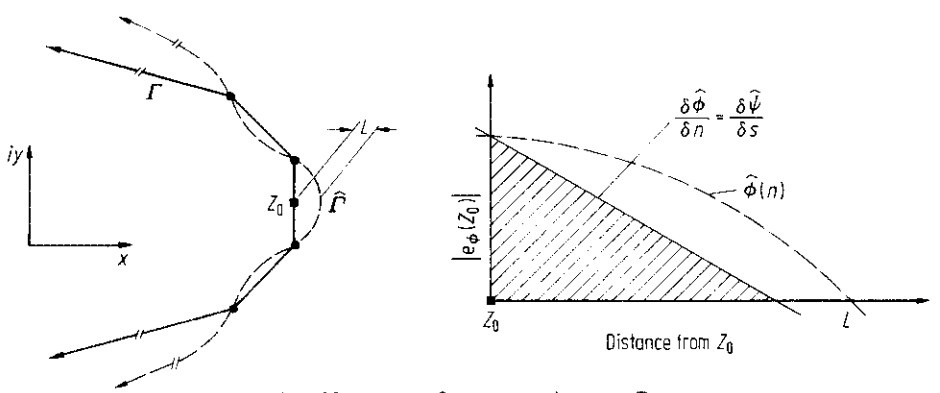

Fig. 22. Area of error at point $z_0 \in \Gamma$

Table 1. Comparison of CVBEM error evaluation methods

Method number	1	2	3	4
Error analysis approach	Relative error of known boundary condition	Approximate boundary	Error area	Total relative error
Collocation point locating criteria	Maximum value of error	Maximum departure between $\hat{\Gamma}$ and Γ	Maximum point area of error	Maximum value of error
Computational effort	Single point evaluation of $\hat{\omega}(z)$	Iteration of $\hat{\omega}(z)$ for each point of $\hat{\Gamma}$	4 to 6 evaluations of $\hat{\omega}(z)$ for Γ_j	Single point evaluation of $\hat{\omega}(z)$
Representation of error	Relative error plot of boundary condition match	Plot of $\hat{\Gamma}$ for comparison with Γ	Plot of relative error area along Γ	Plot of total relative error $\lvert G(z) - \hat{\omega}(z)\rvert$
CVBEM class type used of estimate of unknown nodal values	II	I	II	II
Evaluation of $\hat{\omega}(z)$ at nodes	Yes	No	Yes	Yes
Evaluation of $\hat{\omega}(z)$ at points within Γ_j	No	About 4 to 6	No	No
Includes contributions of both harmonic functions	No	No	Yes	Yes
Approximate ratio of computational effort with Method 1	100%	1700%	120%	110%

Table 1 summarizes the main features of the four methods presented. Included in the table are estimates of the computational effort (in CPU time) expressed as a ratio of the considered technique versus Method 1. It is noted that although Method 2 (approximate boundary) generates an easy-to-interpret representation of the CVBEM error, it requires a considerable computational effort.

The various methods for locating additional nodal points on Γ is demonstrated by application of the CVBEM for solving a potential problem. The analytic solution to this problem is included in the geometry of Fig. 23. The solution satisfies the Laplace equation and is defined as a function of a local coordinate x–y system with an origin specified as shown in the figure. On the problem boundary, Γ, the potential function is a continuous function of position defined by

$$\phi(z \in \Gamma) = \tfrac{1}{2}(x^2 + y^2). \tag{92}$$

From (92) the boundary conditions are not level curves; consequently, the determination of an approximate boundary $\hat{\Gamma}$ (for Method 2) requires further definition. For this example problem, $\hat{\Gamma}$ is located by using the condition

$$\hat{\Gamma} \equiv \{z : \hat{\phi}(z) = \tfrac{1}{2}(x^2 + y^2) = \tfrac{1}{2}|z|^2\}. \tag{93}$$

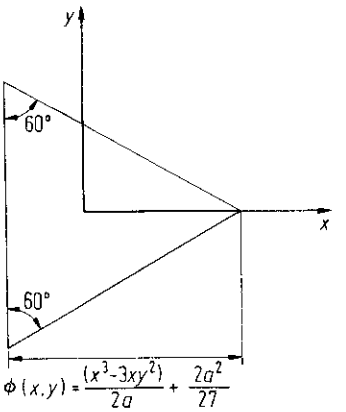

Fig. 23. Application problem geometrics and exact solutions for temperature, $\phi(x, y)$

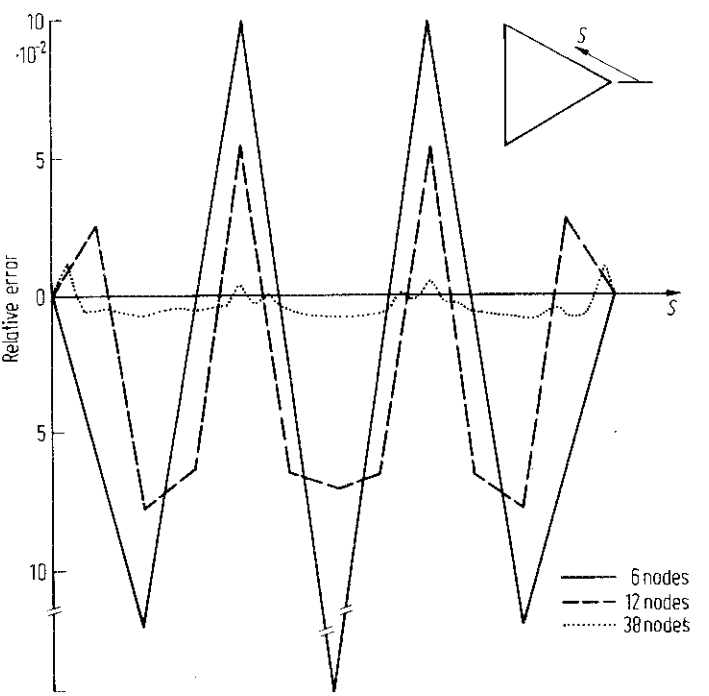

Fig. 24. Boundary relative error plot (Method 1)

Figures 24 through 27 illustrate the several error evaluation methods for 3 nodal placements (evenly spaced).

From the figures, Methods 1, 3, and 4 provide similar abstract representations of the CVBEM modeling error. However, Method 2 results in a visual representation of approximation error which is easily interpretable. Often it can be argued that the precise mathematical description of the problem boundary is not achieved due to

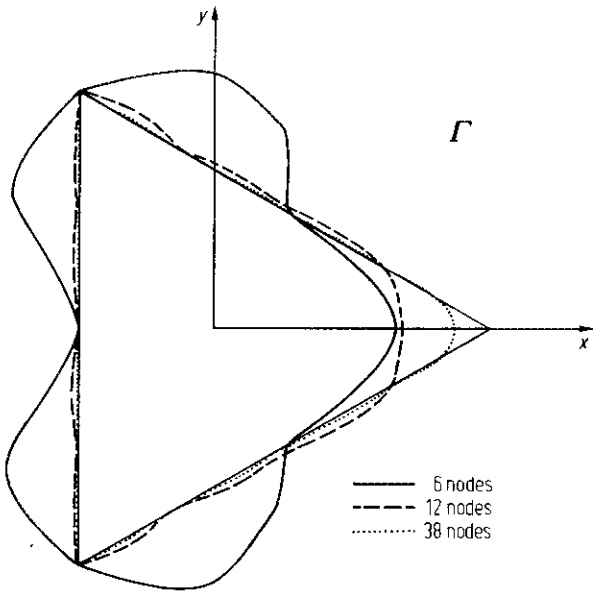

Fig. 25. Approximative boundaries for three nodal point distributions (Method 2)

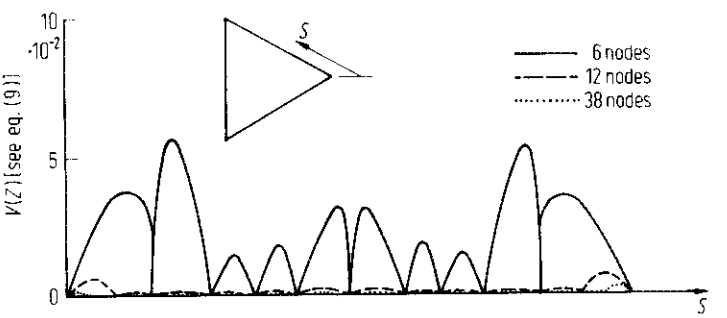

Fig. 26. Area error plot along boundary (Method 3)

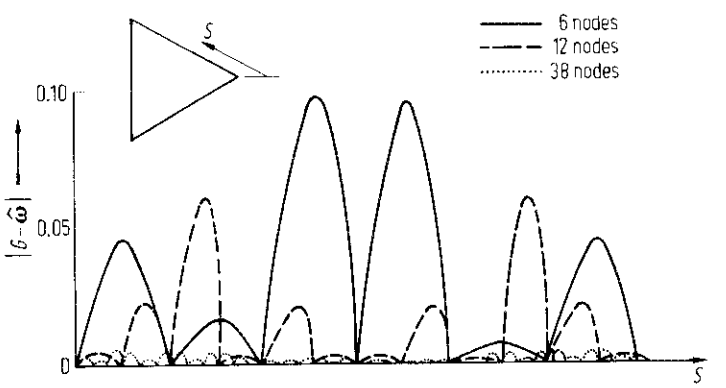

Fig. 27. Trial function error plot along boundary (Method 4)

the construction of the prototype, and that the approximate boundary $\hat{\Gamma}$ may actually represent a more probable end product. Because $\hat{\omega}(z)$ is the exact solution of the boundary value problem with Γ transformed into $\hat{\Gamma}$, then the selection of a $\hat{\Gamma}$ has the advantage of also being associated with the generating $\hat{\omega}(z)$ solution.

7.12 Sources and Sinks

Let $\Omega \cup \Gamma \in P$. Then the CVBEM develops a function $\hat{\omega}_k(z)$ analytic on Ω and continuous on Γ (for $k \geqq 0$). Let $f_i(z)$ be analytic on Ω. Then

$$F(z) = \hat{\omega}_k(z) = \sum_{i=1}^{k} f_i(z) \tag{94}$$

is analytic on Ω for k, a finite integer.

Let $\omega(z)$ be an analytic function on $\Omega \cup \Gamma$ except at points $z_i \in \Omega$ where there exist sources or sinks. A CVBEM approximation of $\omega(z)$ is determined by

$$F(z) = \hat{\omega}_k^*(z) + \sum_{i=1}^{k} (-S) \ln (z - z_i) \tag{95}$$

where $z_i \in \Omega$, S is the strength of the source, and $\hat{\omega}_k^*(z)$ is a CVBEM approximation function determined by approximating the modified boundary condition values of $\omega(z) + \sum S \ln (z - z_i)$ on Γ.

To illustrate the source (sink) function, let point $z_i = x_i + \mathrm{i}\, y_i \in \Omega$. Let z be a point in Ω and define the radial coordinates

$$z - z_i = R e^{i\theta}: \quad R > 0, \quad 0 \leqq \theta < 2\pi . \tag{96}$$

At a radial distance R_0 from z_i, the circumference is $2\pi R_0$. The unit flux (unit flow per unit cross-section length) in the R-direction is given by

$$q = -K \frac{\partial \phi}{\partial R} \tag{97}$$

where K is a transport coefficient. Then the total flow away from point z_i at a distance of R_0 is

$$Q(R_0) = \left(-K \frac{\partial \phi}{\partial R}\bigg|_{R_0} \right) (2\pi R_0) . \tag{98}$$

For $Q(R_0)$ assume a constant value $Q(R_0) = Q$,

$$-\frac{Q}{2\pi K} = \left(R \frac{\partial \phi}{\partial R} \right)\bigg|_{R_0}, \quad R_0 > 0 . \tag{99}$$

Let $S = Q/(2\pi K)$. Then

$$-S \frac{dR}{R} = d\phi \tag{100}$$

where it is noted that $\phi(\theta, R) = \phi(R)$ due to symmetry of flow from point z_i. Then

$$-S \ln R = \phi(R). \tag{101}$$

Similarly, a sink is defined as a negative source by

$$S \ln R = \phi(R). \tag{102}$$

Thus a flow field containing k sources and sinks described by the analytic function

$$F^*(z) = -\sum_{i=1}^{k} S \ln (z - z_i). \tag{103}$$

The function $F^*(z)$ of (103) imposes complex values on boundary Γ. The objective is to approximate $\omega(z)$ on $\Omega \cup \Gamma$ where $\omega(z)$ contains $F^*(z)$. For instance, the domain $\Omega \cup \Gamma$ may also be subjected to other effects such as linear flow, corners, and other possibilities. However we do know values of $\omega(z)$ along the boundary Γ which include the effects of $F^*(z)$. Thus, to approximate $\omega(z)$ on $\Omega \cup \Gamma$, the CVBEM is used to determine a $\hat{\omega}_k^*(z)$ which approximates $[\omega(z) - F^*(z)]$ on Γ.

7.13 Regional Inhomogeneity

Figure 28 illustrates the case of two dissimilar materials with conductivities K_1 and K_2, for steady state conditions, two conditions are satisfied along the interface; namely 1) the potential ϕ is a boundary condition for both domains Ω_1 and Ω_2, and 2) the normal flux $\partial\phi/\partial n$ values are equal for Ω_1 and Ω_2.

The CVBEM is used for the problem of Fig. 28 by developing two approximations, one for each of Ω_1 and Ω_2, such that the specified and interface boundary conditions are both satisfied. The error of the approximations can be evaluated using the approximate boundary approach where special attention is paid towards the two approximate boundaries (from Ω_1 and Ω_2) developed along the interface.

Because the CVBEM results in square, fully-occupied matrix systems, the analysis of multiple regions can result in very large matrix systems. Consequently, the CVBEM may become computationally inefficient when dealing with domains composed of several dissimilar materials.

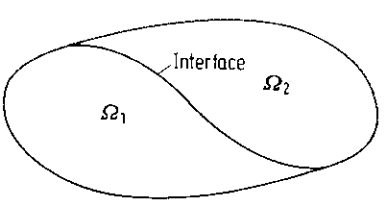

Fig. 28. Dissimilar materials problem

7.14 The Poisson Equation

The two-dimensional Poisson equation on domain Ω is given by

$$\nabla^2\phi = f(x, y), \quad (x, y) \in \Omega \tag{104}$$

where $\phi(x, y)$ is a potential function and $f(x, y)$ is a prescribed function of (x, y) coordinates. Given boundary conditions on the simple closed boundary Γ (enclosing the simply connected domain Ω), the CVBEM can be extended to approximate the boundary value problem of (104).

Let $\phi_p(x, y)$ be a particular solution of (104). Let $\hat{\omega}^*(z)$ be a CVBEM approximation of the Laplace equation $\nabla^2\phi = 0$ where boundary conditions on Γ are specified by subtracting the value of $\phi_p(x, y)$ for $(x, y) \in \Gamma$. That is, determine $\hat{\omega}^*(z)$ on $\Omega \cup \Gamma$ such that $\Delta\xi_k^*$ are the boundary conditions given by

$$\Delta\xi_k^* = \Delta\xi_k - \phi_p \Big|_{\Gamma}. \tag{105}$$

Then necessarily $\hat{\omega}^*(z) = \hat{\phi}^*(z) + i\,\hat{\psi}^*(z)$, and the CVBEM solution to the boundary value problem of (104) with boundary conditions $\Delta\xi_k$ on Γ is

$$\phi(z) = \phi_p(z) + \hat{\phi}^*(z), \quad z \in \Omega. \tag{106}$$

The above modeling approach is outlined by the following steps:

1. Find $\phi_p(z) = \phi_p(x, y)$ such that $\nabla^2\phi_p = f(x, y)$.
2. Evaluate $\Delta\xi_k^* = \Delta\xi_k - \phi_p(x, y)$ for $(x, y) \in \Gamma$.
3. Develop $\hat{\omega}^*(z)$ based on $\Delta\xi_k^*$ boundary conditions.
4. Develop error analysis based on the solution of step 3.
5. Construct the CVBEM solution $\omega(z)$ by adding, $\omega(z) = \omega^*(z) + \phi_p(z)$.
6. CVBEM solution to (104) is $\phi(z) = \hat{\phi}^*(z) + \phi_p(z)$.

It is seen from the above methodology that the approximation of the Poisson equation is simply the application of the CVBEM to a Laplace problem with modified boundary conditions. Consequently, an important step to this solution technique is the development of a particular solution, $\phi_p(x, y)$. The following Table 2 provides a few basic particular solutions. It shold be noted that an infinity of particular solutions are possible for each $f(x, y)$.

Table 2. Particular solutions of the Poisson equation

$f(x, y)$	$\phi_p(x, y)$
k	$k\,x^2/2$
k	$k\,y^2/2$
k	$k\,(x^2 + y^2)/4$
$k\,x$	$k\,x^3/6$
$k\,y$	$k\,y^3/6$
$a\,p(p-1)\,x^{p-2} + b\,q(q-1)\,y^{q-2}$	$a\,x^p + b\,y^q$

7.15 Computer-Aided-Analysis and the CVBEM

The CVBEM can be used in a computer-aided-design environment where the engineer or scientist idenifies additional boundary element nodal point locations based on computer errors in satisfying the known boundary conditions. In this fashion, the analyst develops a problem geometry which is acceptable for prototype construction, and the CVBEM approximation determines the exact solution for the potential problem defined over this prototype geometry. Because the computer interactive technique uses graphical displays, the approach is efficient and easy to use.

In the previous chapter, the CVBEM has been shown to be a powerful tool for the numerical analysis of Laplace or Poisson equation boundary value problems. The numerical approach is to discretize the boundary Γ by nodal points into boundary elements (Fig. 29), and then specify a continuous global trial function $G(\zeta)$ on Γ as a function of the nodal values. Using the Cauchy integral, the resulting integral equation is

$$\hat{\omega}(z_0) = \frac{1}{2\pi i} \int_{\Gamma} \frac{G(\zeta)\, dz}{\zeta - z_0} \tag{107}$$

where $\hat{\omega}(z_0)$ is the CVBEM approximation for $z_0 \in \Omega$; and Ω is a two-dimensional simply connected domain enclosed by the simple closed contour Γ.

Because $G(\zeta)$ is continuous on Γ, then $\hat{\omega}(z)$ is analytic over Ω and can be written as the sum of two harmonic functions

$$\hat{\omega}(z) = \hat{\phi}(z) + i\,\hat{\psi}(z)\,. \tag{108}$$

Thus both $\hat{\phi}(z)$ and $\hat{\psi}(z)$ exactly satisfy the Laplace equation over Ω.

Approximation error occurs due to $\hat{\omega}(z)$ not satisfying the boundary conditions on Γ exactly. However, an approximate boundary $\hat{\Gamma}$ can be developed which represents the location where $\hat{\omega}(z)$ equals the specified boundary conditions such as level curves. Consequently, the CVBEM approximation error can be interpreted as a transformation of $\Gamma \to \hat{\Gamma}$ where the ultimate objective is to have $\hat{\Gamma}$ coincide

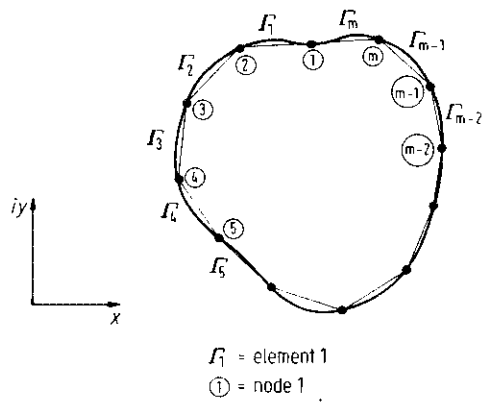

Fig. 29. Modeling Γ by boundary elements Γ_j

with Γ. Because all the error of approximation is due to incorrect boundary element trial functions, accuracy is increased by the addition of boundary nodal points where approximation error is identified to be large (i.e., adaptive integration).

As $\hat{\Gamma}$ approaches Γ geometrically, the analyst is assured by the Maximum Modulus Theorem that the maximum approximation error occurs on Γ and that the governing partial differential equation (Laplace) is solved exactly. Consequently, the final product is the exact solution for a problem geometry which is the construction tolerance for the prototype construction.

Generally, the types of numerical approximation errors in solving potential problems is of two forms: (i) errors due to not satisfying the governing equation over Ω, and (ii) errors due to not satisfying the boundary conditions continuously on Γ. For the CVBEM (and for other boundary integral equation methods), the first type of approximation error is eliminated due to both $\hat{\phi}$ and $\hat{\psi}$ being potential functions. But $\hat{\omega}(z)$ does not usually satisfy the boundary conditions continuously on Γ (if it did, then $\hat{\omega}(z) = \omega(z)$). The next step in the CVBEM analysis is to work with $\hat{\omega}(z)$ in order that $\hat{\omega}(z) \to \omega(z)$.

This step in the analysis of approximation error provides a significant advantage over domain numerical methods such as finite elements or finite differences. In the domain methods, the analyst examines error with a form of vector space Cauchy convergence criteria by arbitrarily increasing the domain nodal densities and comparing the resulting change in estimated nodal values. Whereas with the CVBEM, the analysis has several forms of the approximation error to work with.

The easiest form of error to study is the development of an approximate boundary $\hat{\Gamma}$ which represents the location where $\hat{\omega}(z)$ achieves the problem boundary values of $\omega(z)$. Generally, the boundary conditions are constant values of ϕ or ψ along boundary elements, i.e. $\phi = \phi_j$ for $z \in \Gamma_j$ or $\psi = \psi_k$, for $z \in \Gamma_k$. This set of m nodal values $\{\phi_j, \psi_k\}$ are level curves of $\omega(z)$. The approximate boundary $\hat{\Gamma}$ is determined by locating those points where $\hat{\phi} = \phi_j$ and $\hat{\psi} = \psi_k$. Due to the collocation process, $\hat{\Gamma}$ intersects Γ at least at each nodal location, z_j, $j = 1, 2, \ldots, m$.

To determine $\hat{\Gamma}$, each element Γ_j is further subdivided by interior points where $\hat{\omega}(z)$ is to be evaluated. At each element interior point, $\hat{\omega}(z)$ is calculated from the Cauchy line integral and the values of $\hat{\phi}$ and $\hat{\psi}$ are determined. If the appropriate $\hat{\phi}$ (or $\hat{\psi}$) matches the boundary condition on Γ_j, then $\hat{\Gamma}$ intersects Γ at that point. Otherwise, subsequent points are evaluated by marching pointwise along a line perpendicular to Γ_j until the boundary condition value is reached. For point locations interior of $\bar{\Omega} \cup \Gamma$, an analytic continuation of $\hat{\omega}(z)$ is used.

In this fashion, a set of points is determined where $\hat{\omega}(z)$ equals the desired ϕ_j or ψ_k values. The contour $\hat{\Gamma}$ is estimated by connecting these points with straight lines. Because $\hat{\Gamma}$ and Γ intersect at least at nodal point locations, $\hat{\Gamma}$ appears as a plot which oscillates about the Γ contour.

It is convenient to use a graphical display of both Γ and $\hat{\Gamma}$ superimposed on the CRT. By magnification of the departure between Γ and $\hat{\Gamma}$, the analyst can easily inspect the performance of the CVBEM approximation. Because the approximation error is due to the assumed basis function assumptions, the integration error is reduced by the addition of nodal points on Γ, similar to an adaptive integration technique.

The addition of nodal points can be made directly via the CRT screen and a "locating the closest boundary coordinate" computergraphics subroutine. After the nodal additions are completed, a new $\hat{\omega}(z)$ is determined and the revised $\hat{\Gamma}$ plotted on Γ. By the addition (and deletion) of nodal points from Γ, the analyst is able to quickly evaluate the quality of the CVBEM model. Because the addition of a nodal point can be interpreted as the addition of an approximation error sink term, the geometric representation of error by means of $\hat{\Gamma}$ provides a mathematically sophisticated yet easy-to-use modeling tool.

References

1 Hromadka II, T.V. and Guymon, G.L., Application of a Boundary Integral Equation to Prediction of Freezing Fronts in Soils. In: Cold Regions Science and Technology **6**, 115–121 (1982).
2 Hromadka II, T.V. and Guymon, G.L., Complex Polynomial Approximation of the Laplace Equation. In: ASCE Hydraulics Division, Vol. 110, No. 3, March 1984
3 Hromadka II, V.T. and Guymon, G.L., A Complex Variable Boundary Element Method: Development. International Journal of Numerical Methods in Engineering, April 1983,
4 Hromadka II, T.V., The Complex Variable Boundary Element Method. Springer-Verlag, Berlin, Heidelberg, New York 1984